

Essential Role Played by the C-Terminal Domain of Glycoprotein I in Envelopment of Varicella-Zoster Virus in the *trans*-Golgi Network: Interactions of Glycoproteins with Tegument

ZUO-HONG WANG,¹ MICHAEL D. GERSHON,² OCTAVIAN LUNGU,³ ZHENGLUN ZHU,^{2†}
SUZANNE MALLORY,⁴ ANN M. ARVIN,⁴ AND ANNE A. GERSHON^{5*}

*Institute of Human Nutrition*¹ and *Departments of Anatomy and Cell Biology,*² *Microbiology,*³ and *Pediatrics,*⁵ *College of Physicians and Surgeons, Columbia University, New York, New York 10032,* and *Departments of Pediatrics and Microbiology/Immunology, Stanford University School of Medicine, Stanford, California 94305*⁴

Received 14 August 2000/Accepted 28 September 2000

Varicella-zoster virus (VZV) is enveloped in the *trans*-Golgi network (TGN). Here we report that glycoprotein I (gI) is required within the TGN for VZV envelopment. Enveloping membranous TGN cisternae were microscopically identified in cells infected with intact VZV. These sacs curved around, and ultimately enclosed, nucleocapsids. Tegument coated the concave face of these sacs, which formed the viral envelope, but the convex surface was tegument-free. TGN cisternae of cells infected with VZV mutants lacking gI (gI_Δ) or its C (gI_{ΔC})- or N-terminal (gI_{ΔN})-terminal domains were uniformly tegument coated and adhered to one another, forming bizarre membranous stacks. Viral envelopment was compromised, and no virions were delivered to post-Golgi structures. The TGN was not gI-immunoreactive in cells infected with the gI_Δ or gI_{ΔN} mutants, but it was in cells infected with gI_{ΔC} (because the ectodomains of gI and gE interact). The presence in the TGN of gI lacking a C-terminal domain, therefore, was not sufficient to maintain enveloping cisternae. In cells infected with intact VZV or with gI_Δ, gI_{ΔN}, or gI_{ΔC} mutants, ORF10p immunoreactivity was concentrated on the cytosolic face of TGN membranes, suggesting that it interacts with the cytosolic domains of glycoproteins. Because of the gE-gI interaction, cotransfected cells that expressed gE or gI were able to target truncated forms of the other to the TGN. Our data suggest that the C-terminal domain of gI is required to segregate viral and cellular proteins in enveloping TGN cisternae.

Morphological observations have indicated that nucleocapsids are assembled in the nuclei of cells infected with varicella-zoster virus (VZV) and acquire an envelope from the inner nuclear membrane as they bud from the nucleus into the lumen of the perinuclear cisterna (PC)-rough endoplasmic reticulum (RER) (10, 30). Although they are thus encapsulated, the virions in the PC-RER do not appear to be completely formed because they lack the electron-dense tegument layer that characterizes mature virions. The envelope of these particles, furthermore, does not display glycoprotein E (gE) immunoreactivity and also fails to become radioautographically labeled when cells are incubated with [³H]mannose (10). Since glycoproteins become N-glycosylated cotranslationally (19), these data suggest that the envelope provided by the inner nuclear membrane may be a temporary one that does not contain the N-glycosylated glycoproteins of the mature viral envelope. The maturation of virions, therefore, requires a mechanism that permits them to acquire a normal complement of tegument and their final envelope.

The process by which the requirements for envelopment are fulfilled has been proposed to be the replacement, during the intracellular transport of virions, of the initial, inner-nuclear-membrane-derived envelope with a new one obtained from the

trans-Golgi network (TGN) (10, 30). An analogous mechanism has been postulated to be involved in the envelopment of pseudorabies virus (33). The glycoproteins of VZV are targeted to the TGN and, in infected cells, all appear to become concentrated within this organelle (30). This sorting implies that TGN targeting signals must be present in the sequences of at least some VZV glycoproteins. Such signals have indeed been identified in the cytosolic domains of gE (1, 2, 36, 37) and gI (31). Unenveloped nucleocapsids are frequently seen in electron micrographs of the cytosol of cells infected with VZV (10). It is likely that these nucleocapsids reach the cytosol because the temporary nuclear-membrane-derived envelope fuses with the membrane of the RER, a phenomenon that can readily be visualized when intracellular transport is slowed or interrupted by incubating cells at low temperature or with brefeldin A (10). The appearance of the TGN changes radically in cells infected with VZV. Sacs of the TGN become flattened and acquire the shape of a “C”, with readily distinguishable concave and convex surfaces. The cytosolic face of the concave surface of these cisternae is distinct because tegument proteins accumulate on it. Because tegument proteins lack a signal sequence, they must be synthesized in the cytosol on free polyribosomes. Even though they are thus not integral membrane proteins, tegument protein could nevertheless concentrate adjacent to the concave face of the C-shaped TGN cisternae by adhering to the cytosolic tails of integral membrane proteins that are restricted to this domain. Nucleocapsids, moreover, adhere to the tegument and both eventually become surrounded by the TGN cisternae as these limbs of the

* Corresponding author. Mailing address: Department of Pediatrics, Columbia University, College of Physicians and Surgeons, 630 W. 168th St., New York, NY 10032. Phone: (212) 305-9445. Fax: (212) 342-5218. E-mail: aag1@columbia.edu.

† Present address: Department of Medicine, Harvard Medical School, Boston, Mass.

TGN "wrapping" cisternae extend and ultimately fuse. The fusion of the extending arms of the C shape completes a sphere, which splits to form two membrane-enclosed structures: an inner enveloped virion and an outer transport vesicle. The viral envelope is derived from the concave surface of the wrapping cisterna, while the convex surface of the same structure gives rise to the membrane of the transport vesicle.

The proposed mechanism of TGN envelopment implies that VZV glycoproteins become segregated within each of the C-shaped wrapping cisternae of the TGN. Since the concave surface of these cisternae is postulated to become the viral envelope, the glycoproteins must specifically become concentrated within it. Tegument may thus bind (directly or via adapters) to the cytosolic domains of viral or other integral membrane proteins of this membrane. In contrast, since the convex surface is thought to become a transport vesicle, this face would be expected to be rich in cellular proteins involved in sorting, transport, and vesicular fusion (26). Specifically, the membrane of the convex face of the wrapping cisternae contains mannose 6-phosphate receptors (10), which may explain the observation that newly enveloped virions are transported from the TGN to late endosomes (prelysosomes) (9). TGN-derived vesicles containing mannose 6-phosphate receptors are preferentially sorted to late endosomes (7, 11, 19, 26, 28).

How the proteins of the viral envelope become differentially sorted from the host proteins of the transport vesicle is unknown. Because the glycoproteins are integral membrane proteins, their segregation must take place within the plane of a membrane, possibly that of TGN wrapping cisternae. Segregation of the glycoproteins could be brought about by protein-protein interactions, either between the glycoproteins themselves (to form rafts) or with organizing peripheral membrane proteins in the cytosol. Disruption of the segregation of viral and cellular proteins within the membranes of the Golgi apparatus and/or the TGN might be expected to cause the processing of carbohydrates to become abnormal. The failure of viral and cellular proteins to segregate properly would be anticipated to alter the organization of the Golgi and/or TGN, as well as the relationship between TGN cisternae and tegument proteins.

It is possible that VZV gI plays a role in the segregation of glycoproteins during the formation of the final viral envelope. Although gI is dispensable, mutants that lack gI form microplaques and exhibit a reduced rate of growth (4, 20). Cells infected with gI-deficient virions form abnormal polykaryocytes with a disrupted organization of nuclei (20). These cells also aberrantly process gE (4). The molecular weight of gE produced in the absence of gI is greater than normal because of an alteration in its glycosylation. gI and gE are known to form a complex with one another in the RER (1, 13, 14, 21, 24). The absence of gI would thus be expected to affect post- rather than cotranslational steps in the glycosylation of gE, most of which occur in the Golgi apparatus (18). The Golgi apparatus, the TGN, and tegument were therefore examined by light and electron microscopic immunocytochemistry in cells infected with VZV gI deletion mutants to test the hypothesis that gI plays an important role in the separation of viral and host proteins and/or the adherence of tegument to the nascent viral envelope. Studies were carried out with VZV mutants that lacked either all of gI or only its N- or C-terminal regions.

ORF10p (5, 6), IE62 (16, 17), and IE63 (8, 12, 15) were investigated because they are thought to be tegument proteins and components of virions. Observations indicated that the TGN wrapping cisternae and viral tegument form abnormal stacks in cells infected with any of the tested gI mutant virions. Envelopment of VZV is thus compromised. The data support the idea that gI plays a role in enabling viral glycoproteins and tegument to become sequestered on the concave face of the C-shaped cisternae that normally envelop VZV in the TGN.

MATERIALS AND METHODS

Cells and infection. Wild-type (a low-passage isolate), Ellen, vaccine (Oka), and mutant forms of VZV were propagated in human embryonic lung fibroblasts (HELFL), as previously described (10). Cells were examined 3 to 5 days after infection. No significant differences were found in the appearance of cells infected with the low-passage isolate, Ellen, or Oka strains but, except for the gI mutant virions, all illustrations are of material infected with Ellen. The VZV mutants were generated from four overlapping fragments of genomic DNA from the Oka strain of VZV ligated into SuperCos 1 cosmid vectors, provided by George Kemble (Aviron, Inc., Mountain View, Calif.) (20). The deficits in these mutants have been demonstrated to be fully reversed by reinfection of gI. MeWo cells infected with mutant virions were sent to New York from California. These cells were used to infect HELFL cells, within which the mutant virions were subsequently propagated. Extremely poor yields of cell-free virus were obtained from cells infected with any of the gI deletion mutants. Microplaques were observed when these mutants were propagated in HELFL, just as previously reported when these mutants were propagated in MeWo cells (20). On the other hand, the multinucleated giant cells that were common in gI mutant-infected MeWo cells were not observed in their HELFL equivalents. In most experiments with the gI mutant virions, therefore, infection was transmitted to fresh cultures with cells rather than with cell-free VZV. The trafficking of gI immunoreactivity in infected HELFL cells was compared with that of gI in transfected Cos-7 cells, which expressed either the full-length gI or a truncated mutant that lacked the N- or C-terminal domain (31). Cos-7 cells were grown at 37°C with 5% CO₂ in Dulbecco modified Eagle medium, containing heat-inactivated 10% fetal bovine serum, 100 U of penicillin per ml, and 100 U of streptomycin per ml. Monoclonal antibodies to gE and gI were purchased from Viro Research, Inc. (Rockford, Ill.).

Transfection. For transfection, cells were grown on glass coverslips in two- or eight-well chambers. Cells were transfected with cDNA constructs using Lipofectin (Life Technologies/GIBCO, Grand Island, N.Y.) according to the manufacturer's directions. Cells were incubated at 37°C in an atmosphere of 5% CO₂. The media were changed after 12 h, and incubation was continued for another 48 h. In most experiments the cells were then fixed with 2% formaldehyde (freshly prepared from paraformaldehyde) in phosphate-buffered saline (PBS) at pH 7.4 for 2 h at room temperature.

Immunocytochemistry. Rabbit polyclonal antibodies to recombinant gE and gI were also utilized (30, 31). Antibodies to detect the adaptin protein complex, AP-1 (monoclonal anti- γ -adaptin clone 100/3), were obtained from Sigma Chemical Co. (St. Louis, Mo.) (2, 27). Fixed cells were washed with PBS and permeabilized with 0.1% Triton X-100 in PBS containing 2.0 mg of bovine serum albumin (BSA) per ml. Primary and secondary antibodies used to visualize proteins by single- and double-label immunocytochemistry were applied as described previously (31). In initial experiments, the secondary antibodies were goat anti-rabbit or anti-mouse immunoglobulin G labeled with fluorescein isothiocyanate (FITC; Kirkegaard & Perry, Gaithersburg, Md.) or cyanine-3 (Cy3; Jackson Immunoresearch Laboratories, Inc., West Grove, Pa.). In subsequent studies, the secondary antibodies were coupled to Alexa fluor-488 or Alexa-594 (Molecular Probes, Inc., Eugene, Oreg.) because of the brighter fluorescence of the newer fluorophores. Slides were examined by vertical fluorescence microscopy (Leica).

Electron microscopy. Cells were fixed with 2.5% glutaraldehyde and postfixed in 1% OsO₄ containing 1% potassium ferrocyanide (9). Following dehydration and clearing, these preparations were embedded in an epoxy resin (Epon 812). For immunocytochemistry, the fixative contained 4% formaldehyde (from paraformaldehyde) and either 0.05 or 0.1% glutaraldehyde in 100 mM sodium phosphate buffer. Residual aldehyde groups were quenched with 50 mM ammonium chloride. Tissues for immunocytochemistry were washed, dehydrated, and embedded in a hydrophilic embedding medium (LR Gold; in a well sandwiched between two layers of ACLAR plastic). The resin was polymerized with UV light

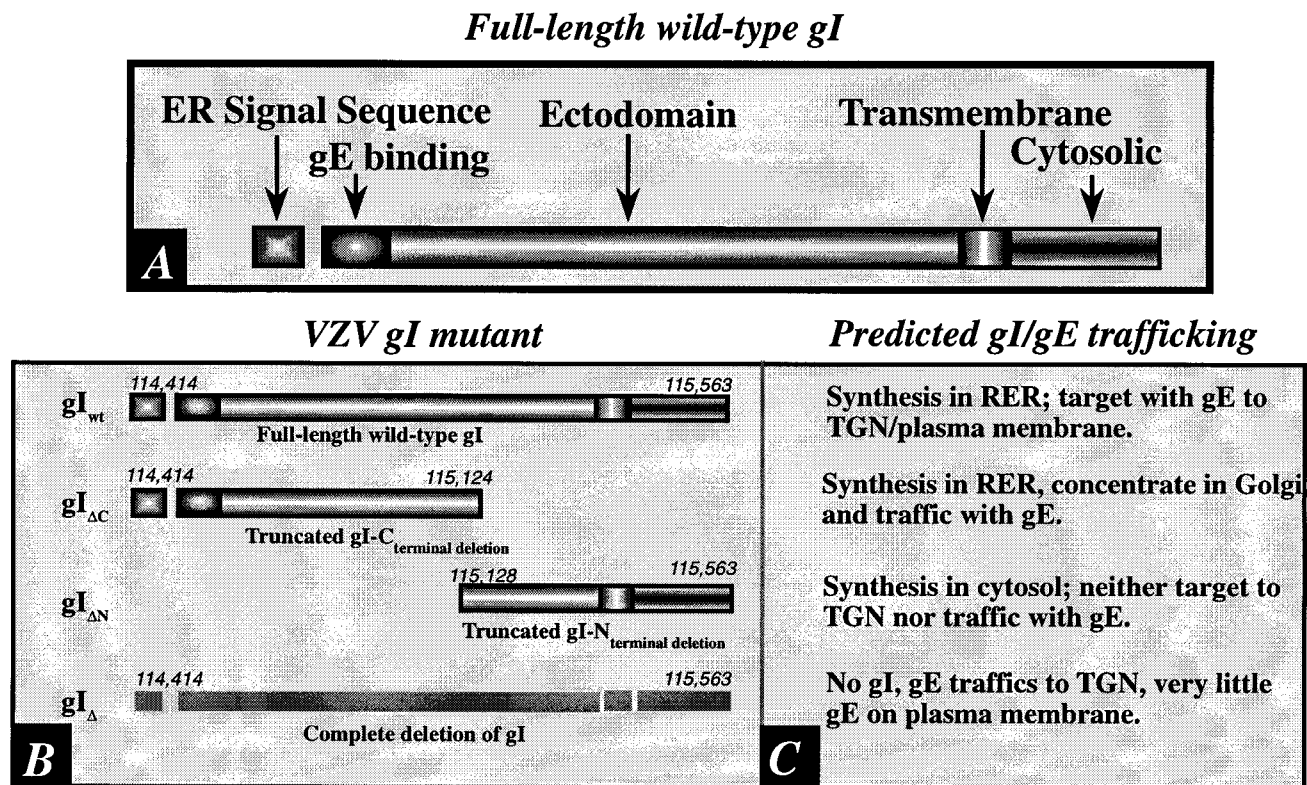


FIG. 1. (A) The domains of *gI* are shown diagrammatically. Note that the signal sequence, which is presumably responsible for the biosynthesis of *gI* in the RER, is at the N-terminal end of the molecule. Because signal peptides are cleaved cotranslationally, this domain is not found in the completed integral membrane protein. (B) The domains of the tested mutant forms of *gI* are compared to those of the full-length intact *gI*. The numbers refer to base pairs in the VZV genome at which the sequence encoding the indicated domain begins or ends. (C) The predicted patterns of *gI* trafficking in cells infected with the corresponding virions diagrammed in panel B. These predictions were tested in immunocytochemical experiments. (i) gI_{wt} . The trafficking of *gI* in cells infected with intact VZV has previously been described (30) and is thus the expected pattern in cells infected with intact virions. Since *gI* and *gE* form a complex in the RER, they would be expected to traffic together during post-RER stages of intracellular transport. (ii) $gI_{\Delta C}$. Despite the deletion of its C-terminal domain, the $gI_{\Delta C}$ mutant protein would still be expected to be synthesized in the RER because it contains a signal sequence; however, since the transmembrane domain is lacking, the $gI_{\Delta C}$ mutant should be completely translocated to the lumen of the RER and lack a membranous anchor. Although $gI_{\Delta C}$ is thus analogous to a secreted protein, the complex formed with *gE* at its N-terminal would be expected to cause the $gI_{\Delta C}$ mutant to be transported along with its normal *gE* partner. (iii) $gI_{\Delta N}$. The deletion of the N-terminal domain of *gI* ($gI_{\Delta N}$) would be anticipated to prevent its biosynthesis in the RER because of the lack of a signal sequence. The deletion of the N-terminal domain of *gI* would also be expected to prevent interactions of $gI_{\Delta N}$ with *gE*. The elimination of these interactions would not be expected to interfere with the targeting of *gE* to the TGN because *gE* has its own TGN targeting sequence and patch (37). (iv) gI_{Δ} . The total deletion of *gI* would, of course, be expected to eliminate *gI* immunoreactivity. Because of the endocytosis signal in the sequence of *gE* (22), relatively little *gE* would be expected to be retained on the plasma membrane unless it were induced to remain there because it is complexed with *gI*. *gI* is not retrieved to the TGN when it traffics to the plasma membrane in transfected cells that express only *gI* (1, 30; but see also reference 21). The retention of *gE* in the plasma membrane might thus occur in cells infected with virions carrying gI_{wt} but not in those carrying $gI_{\Delta N}$ or gI_{Δ} . Because the $gI_{\Delta C}$ protein is not membrane anchored, it also would not be expected to interfere with the endocytosis of the *gE* to which it is bound.

at -20°C . Thin sections were cut and picked up on Formvar-carbon-coated nickel grids. The sections were treated on the grids with a blocking solution containing 1.0% BSA, 0.5% cold-water fish gelatin, and 0.1% Triton X-100 in Tris-buffered saline for 60 min at room temperature. The sections were then incubated with antibodies to *gI*, *gE*, or ORF10 as specified below. Grids were subsequently washed and incubated 3 h at room temperature with goat anti-rabbit or anti-mouse secondary antibodies coupled to 5- or 10-nm particles of colloidal gold (diluted 1:20 with blocking solution; Amersham Corp., Arlington Heights, Ill.). Grids were examined in a JEOLCO JEM 1200 EX electron microscope.

RESULTS

Immunocytochemical localization of *gI* and *gE* in cells infected with *gI* mutants. Light and electron microscopic immunocytochemistry were employed to study the targeting of *gI*

and *gE* in cells infected with intact VZV and in cells infected with *gI* mutant virions. The production and characterization of these mutants have previously been described (20). The mutations that were studied are illustrated in Fig. 1. The experiments were designed to test predictions about patterns of trafficking of *gI* and *gE* in cells infected with the mutant virions. These predictions were based on the assumptions that *gI* and *gE* interact at the N-terminal domains of the molecules and that a complex of these two proteins is formed in the RER (1, 13, 14, 21, 24). The sorting of *gI* has previously been studied at the light microscopic level, both in infected cells (20, 30) and in transfected cells expressing only *gI* (1, 31, 34). Nevertheless, the effects of deleting *gI*, or particular regions of the molecule, on the structure of the TGN, the concentration of other gly-

coproteins within the TGN, and the distribution of tegument have not previously been investigated.

When cells were infected with intact VZV, both gE (Fig. 2A and C) and gI (Fig. 2B and C) were concentrated in the TGN where they were co-localized. The TGN was identified as described previously (31), either by using the fluorescence of the lipid, *N*-(ϵ -7-nitrobenz-2-oxa-1,3-diazo-4-yl-aminocaproyl)-D-erythro-sphingosine (C_6 -NBD-ceramide) (25) or antibodies to γ -adaptin (2, 27) as markers (data not illustrated). The immunoreactivities of both proteins were also located in the plasma membrane ($gI > gE$). The complete deletion of gI (gI_{Δ}) did not affect the localization of gE in the TGN (Fig. 2D and F) but, as expected, no gI immunoreactivity could be detected in cells that were infected with gI_{Δ} mutant virions (Fig. 2E and F). The immunoreactivities of both gE (Fig. 2G and I) and gI (Fig. 2H and I) were evident when cells were infected with a mutant gI lacking the C-terminal domain ($gI_{\Delta C}$). Again, as in cells infected with the intact VZV, a coincident localization of both gE and gI was found in the TGN. The plasma membrane localization of gI (Fig. 2H), however, was less evident in cells infected with the $gI_{\Delta C}$ mutant than was the case in cells infected with intact VZV (compare Fig. 2B with Fig. 2H). When the N-terminal region of gI was deleted ($gI_{\Delta N}$), gE still became concentrated in the TGN (Fig. 2J and L); however, very little gI was seen in the $gI_{\Delta N}$ -infected cells (Fig. 2K). In particular, no gI immunoreactivity could be detected in the TGN, plasma membrane, or any other organelle.

Mutations in gI affect the envelopment of VZV. HELF cells infected with intact VZV were examined electron microscopically as a control to permit possible changes in envelopment and/or intracellular transport caused by mutations in gI to be identified. HELF cells were also infected with the mutant virions illustrated in Fig. 1 and were processed in a manner that was identical to that used for the analysis of the control cells infected with intact VZV, so that the two types of infected cells could be compared. As previously reported (10), the PC-RER (Fig. 3A) was found to contain enveloped virions in the control cells infected with intact VZV. The structure of the particles in the PC-RER, however, differed from that of mature enveloped virions in that a clear zone was present in the space between the viral envelope and the nucleocapsid, where electron-dense tegument is normally found. (Compare the structure of the virions in the PC-RER [Fig. 3A] with that of the virions found in post-TGN vacuoles [Fig. 3D]). The envelope of the PC-RER-located virions, moreover, could readily be distinguished from that of the adjacent cellular membranes of the RER or nuclear envelope. The viral envelope membrane was more electron dense, slightly thicker, and more sharply defined than the cellular membranes. When cells were incubated for 20 min at 20°C, many profiles of virions fusing with the membranes of the RER became evident (Fig. 3B). Following fusion, the viral envelope, which could easily be distinguished from that of the RER (because of its higher electron density and greater thickness) became incorporated into the RER, providing access to cytosol for unenveloped nucleocapsids. The domains of the incorporated viral envelopes distorted the contour of the RER, leaving a semicircular indentation (concave surface facing the cytosol) at the site of fusion.

Unenveloped nucleocapsids were abundant in the cytosol of cells infected with intact VZV (Fig. 3C) and, in the region of

the TGN, these nucleocapsids were associated with curvilinear C-shaped membranous sacs (Fig. 3C and Fig. 4A to C). The membranes of these C-shaped cisternae have previously been demonstrated to display TGN markers and thus to be derived from that organelle (10). In most of the nucleocapsid-cisternal complexes, the nucleocapsids were separated from the concave face of the cellular membranes by electron-dense material that resembled tegument. Varying stages in the wrapping of the C-shaped cellular cisternae around nucleocapsids were identified, leading ultimately to the elimination of the portion of the C shape open to the cytosol by the fusion of the extending arms of the C shape (Fig. 4). This fusion and subsequent fission led to the production of an enveloped virion (Fig. 4D) within a tightly fitting vesicle. The concave tegument-coated face of the original C-shaped membranous sac thus appears to provide the viral envelope, while the outer tegument-free convex membrane provides the vesicle within which the nascent virion is initially contained. Despite their solitary enclosure in a small vesicle at the time of their formation in the TGN, most of the enveloped virions seen in the same cells were located in large, irregularly shaped vacuoles, each of which contained multiple virions (Fig. 3D). These vacuoles have previously been identified as late endosomes-prelysosomes because of their acidic interiors (10) and accessibility within 1 h to a fluid-phase extracellular marker protein (9). Late endosomes are post-TGN structures. Since both the membranes of late endosomes-prelysosomes and those of the vesicles that enclose individual virions within TGN contain mannose 6-phosphate (Man 6-P) receptors (10), it is likely that the virion-containing vesicles that form in the TGN deliver their contents to the late endosomes-prelysosomes where the virions accumulate. Most of the virions in the late endosomes-prelysosomes are pleomorphic and are degraded in their morphology (Fig. 3D). A final characteristic of the VZV-infected cell is a proliferation of smooth membranes in the form of a tubulovesicular network that is continuous with the RER (Fig. 3D).

The ultrastructural appearance of cells infected with each of the gI mutants (gI_{Δ} , $gI_{\Delta C}$, and $gI_{\Delta N}$; Fig. 1) was strikingly different from that of cells infected with intact VZV (compare Fig. 5 with Fig. 3). The morphology of the cells infected with any one of the gI mutants, however, could not be distinguished from that of cells infected with another. The major differences between the morphology of cells infected with the gI mutant virions and that of cells infected with intact VZV lay in the absence of virus-containing late endosomes-prelysosomes and a striking alteration of the Golgi regions of cells infected with the gI mutants (Fig. 5). Because the large accumulations of virions in late endosomes-prelysosomes, which characterized cells infected with intact virions (Fig. 3D), were never seen in cells infected with the gI_{Δ} , $gI_{\Delta C}$, or $gI_{\Delta N}$ mutants, cytoplasmic virions were often difficult to find. The presence of nuclear nucleocapsids was therefore used as a marker to identify cells that were infected with the gI mutants.

In cells that contained relatively small numbers of nucleocapsids in their nuclei and were thus thought to be associated with minimal or early infection, irregularly dilated vacuoles with thickened membranes were found in the *trans* portion of the Golgi apparatus (Fig. 5A). In the same cells, there was little or no associated change in the morphology of the *cis*-Golgi or the stacks of Golgi cisternae (Fig. 5A). At higher magnification

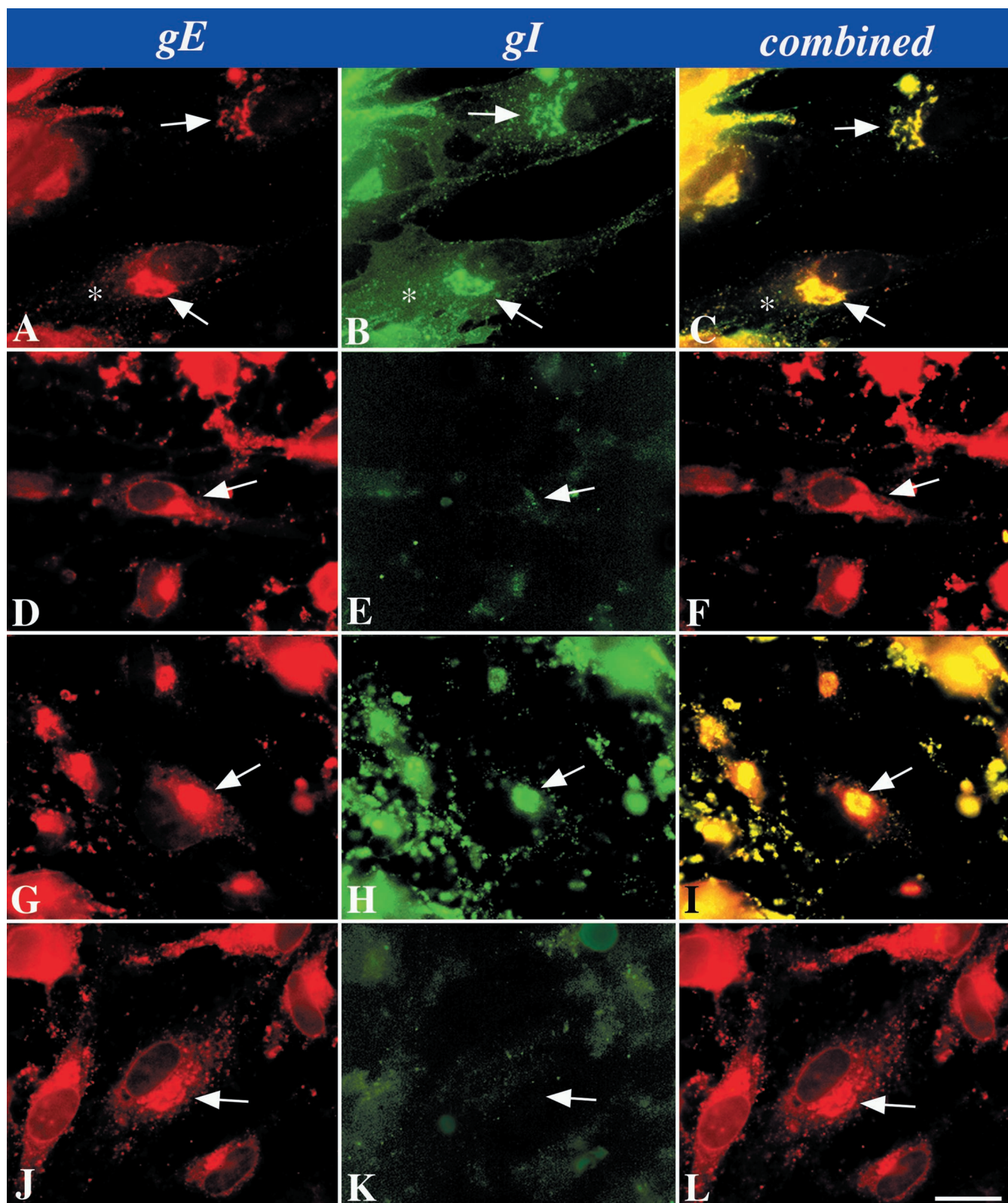


FIG. 2. Immunocytochemical localization of gI and gE immunoreactivities in cells infected with intact (Ellen) or mutant VZV as shown in Fig. 1. (A to C) Wild-type VZV. (D to F) gI_{Δ} . (G to I) $gI_{\Delta C}$. (J to L) $gI_{\Delta N}$. The arrows point to the location of the TGN in the infected cells. The asterisk indicates plasma membrane immunostaining. Bar, 10 μ m.

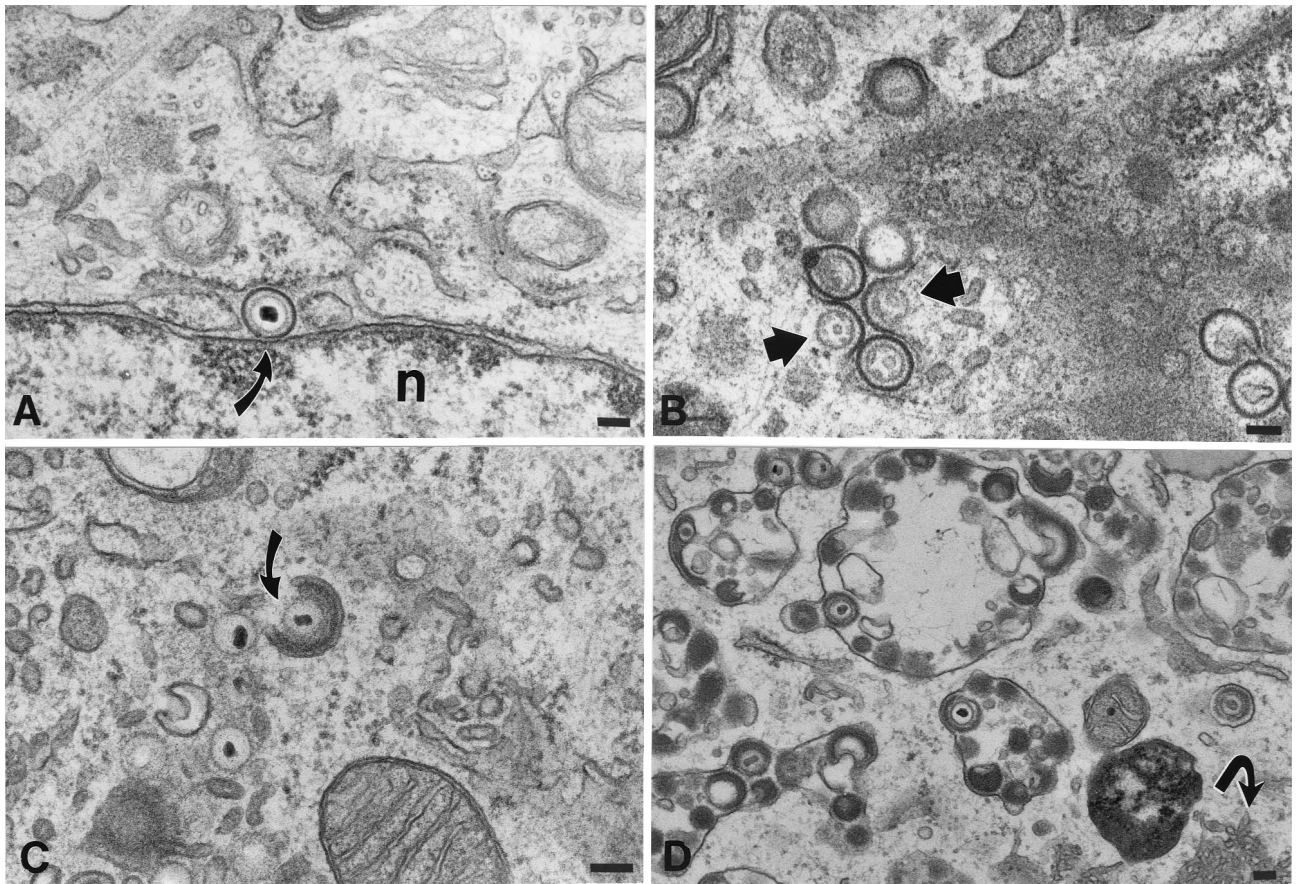


FIG. 3. Cellular locations of nucleocapsids and enveloped virions in HELF cells infected with intact (Ellen) VZV. (A) An enveloped virion lies in the PC-RER (arrow). The virion is located at a point where the RER is continuous with the outer membrane of the nuclear envelope. The thickness and electron density of the viral envelope are greater than those of adjacent cellular membranes. n, nucleus. (B) Enveloped nucleocapsids in the RER fuse with RER membranes, releasing unenveloped nucleocapsids into the cytosol (arrows). The infected cells were incubated at 20°C in order to slow the intracellular transport of VZV. (C) A nucleocapsid in the region of the TGN is partially wrapped by a C-shaped cisterna of cellular membranes (arrow). Note the presence of dense material between the nucleocapsid and the inner, concave face of the wrapping cisterna. Unenveloped nucleocapsids are present in the neighboring cytosol. (D) Enveloped VZV accumulates in large vacuoles that have been found to be late endosomes-prelysosomes. Note also the proliferation of smooth cellular membranes, which are in continuity with the RER (arrow). Bars, 150 nm.

and in cells that contained greater numbers of nuclear nucleocapsids, the apparent thickening of vacuolar membranes could be seen to be due to a coating of the TGN membranes with an amorphous electron-dense material (Fig. 5B). The abnormal vacuoles in the TGN assumed a number of bizarre shapes but often appeared flattened and adherent to one another, forming stacks (Fig. 5B) and evenly spaced concentric rings (Fig. 5C). These stacks and rings consisted of alternating light (electron-lucent) regions, which corresponded to the lumens of flattened cisternae, and dark (electron-dense) layers, which corresponded to the amorphous material that coated the vesicles. The amorphous coating material thus appeared to “glue” adjacent cisternae together to give rise to the stacks and concentric rings of flattened cisternae. In cells that were very highly infected (contained many nuclear nucleocapsids), the entire TGN region was enlarged and assumed a structure that looked like a honeycomb containing many chambers. The walls of these chambers consisted of membranes coated with dense osmiophilic material, while their dilated interiors were electron lucent (Fig. 5D). Tegument-covered nucleocapsids and pleo-

morphic enveloped virions were found within the chambers. The appearance of the osmiophilic material coating the walls of the chambers of the TGN “honeycomb” was indistinguishable from that of the tegument around viral nucleocapsids. The osmiophilic material was found on the cytosolic face of the membranes it coated.

Location of gE and gI immunoreactivities in the TGN cisternae of cells infected with gI_{Δ} , $gI_{\Delta C}$, and $gI_{\Delta N}$ mutant virions. Electron microscopic immunocytochemistry was used to identify the abnormal structures found in the TGN region of cells infected with gI_{Δ} , $gI_{\Delta C}$, and $gI_{\Delta N}$ mutant virions. Postembedding labeling with 10-nm particles of colloidal gold was used to demonstrate the immunoreactivities of gE or gI. Abundant gE immunoreactivity was found in the membranes, stacks, and rings of cisternae in the TGN of cells infected with any of the gI mutants (Fig. 6A). In the highly infected cells, within which the TGN region appeared to be transformed into a honeycomb, gE immunoreactivity was found both in the membranes that lined the chambers and in the envelopes of the virions trapped inside of them (Fig. 6B). No gI immunoreac-

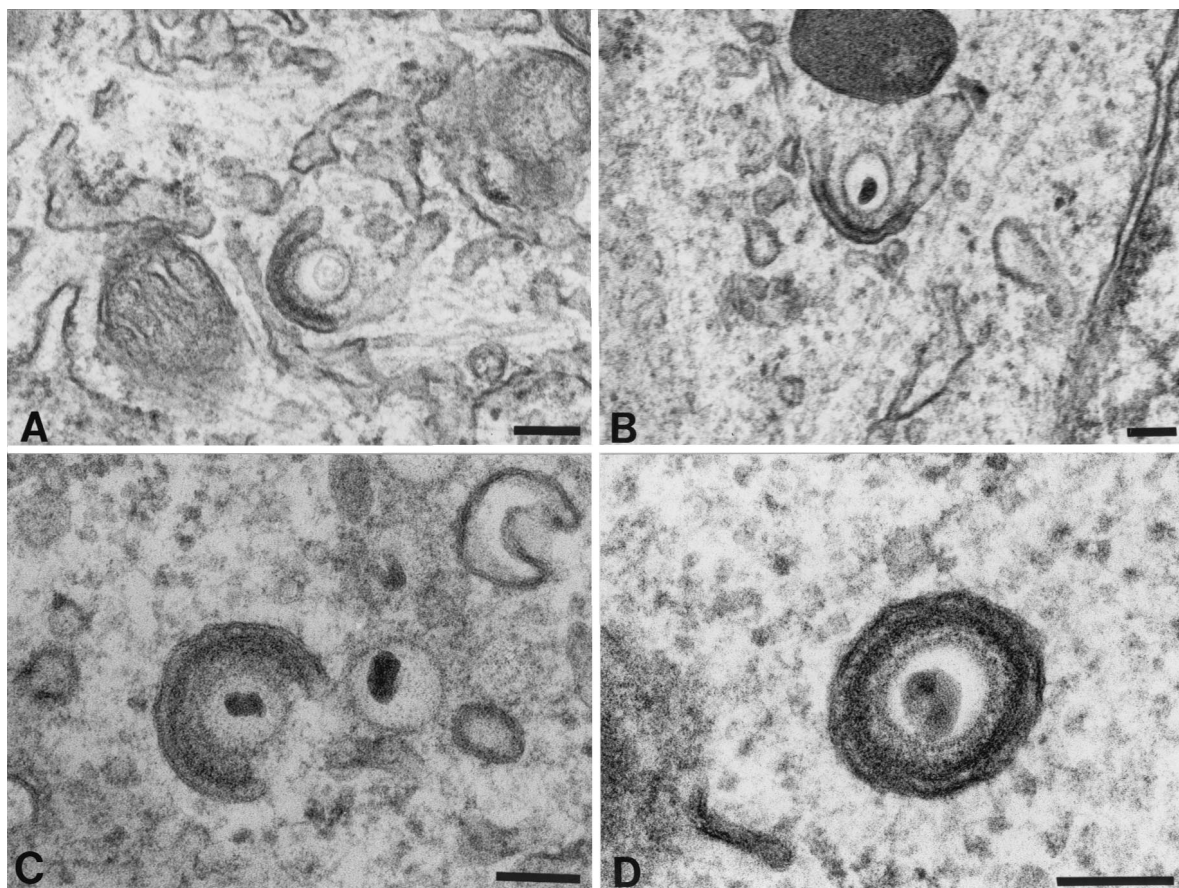


FIG. 4. Apparent stages in the envelopment of VZV in the TGN of cells infected with intact (Ellen) VZV. (A) An unenveloped nucleocapsid makes contact with a specialized C-shaped cisterna of the TGN. Electron-dense material that resembles tegument accumulates between the nucleocapsid and the concave face of the wrapping cisterna. (B and C) The arms of the "C" of the wrapping cisterna extend toward one another, eliminating the space open to the cytosol and gradually enclosing more and more of the nucleocapsid. The electron-dense material remains adherent to the concave face of the wrapping cisterna. (D) The opening to the cytosol has been closed. Two membranes surround the nucleocapsid. The inner membrane has electron-dense tegument-like material adherent to it. The structure is interpreted to be a newly enveloped virion enclosed in a transport vesicle. The inner membrane is in contact with tegument and is derived from the concave face of the original C-shaped cisterna. The outer membrane, that of the transport vesicle, is derived from the convex face of the C-shaped cisterna. Bars, 150 nm.

tivity was seen in cells infected with virions from which gI was deleted (gI_{Δ} ; data not illustrated); however, gI immunoreactivity was observed in the membranes of the aggregated stacks and rings of cisternae in the TGN region of cells infected with the $gI_{\Delta C}$ mutant (Fig. 6C). In doubly labeled preparations of cells infected with the $gI_{\Delta C}$ mutant virus, the membranes of the abnormal vacuoles and cisternae of the TGN displayed coincident localization of gE and gI immunoreactivities (Fig. 6D). There was more gE than gI immunoreactivity in both the singly and the doubly labeled $gI_{\Delta C}$ material (Fig. 6C and D). Neither gE nor gI immunoreactivities were reproducibly associated with the dense material that coated the cytosolic faces of the viral glycoprotein-containing TGN membranes. In contrast to the TGN cisternal membranes of cells infected with the $gI_{\Delta C}$ mutant virus, those of cells infected with $gI_{\Delta N}$ contained only gE immunoreactivity (Fig. 7A). No gI immunoreactivity could be found associated with any membrane in the $gI_{\Delta N}$ -infected cells. The gE immunoreactivity of the cells infected with the $gI_{\Delta N}$ virus was confined to membranes and was not found in the dense material that coated the cytosolic face of these membranes or in the cytosol itself. The cells infected with the $gI_{\Delta N}$

virus did display small amounts of gI immunoreactivity (Fig. 7B); however, in contrast to cells infected with $gI_{\Delta C}$, this immunoreactivity was restricted to the cytosol of $gI_{\Delta N}$ -infected cells.

Coexpression with gI causes ORF10p to concentrate in the TGN. Because tegument is incorporated into virions during envelopment in the TGN, we investigated the possibility that an interaction with a glycoprotein causes a tegument protein to become concentrated in the TGN. ORF10p was selected for study because it is a tegument protein that becomes incorporated into virions (5, 6), and gI was investigated because it contains a TGN retention signal (T^{338}) (31). When expressed by itself in transfected cells ORF10p immunoreactivity was found to be diffusely located throughout the cytoplasm (Fig. 8A and B). In contrast, in cotransfected cells that express both gI and ORF10p, the immunoreactivities of both proteins were strikingly colocalized in the TGN (Fig. 8C and D). These observations are consistent with the idea that ORF10p interacts with gI and that as a result of this glycoprotein-tegument protein interaction, ORF10p is translocated to the TGN.

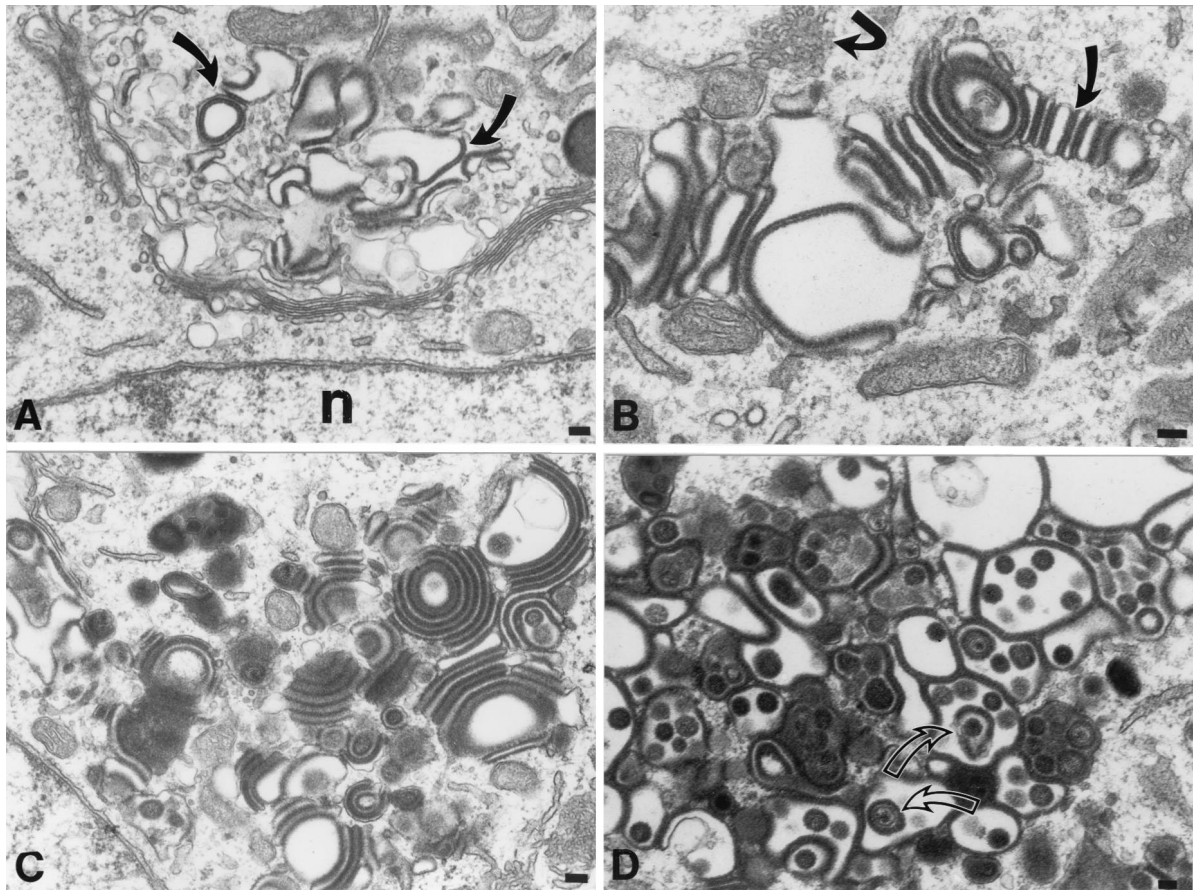


FIG. 5. The morphology of the TGN of cells infected with a mutant VZV in which the C-terminal portion of gI has been deleted ($gI_{\Delta C}$) is different from that of cells infected with intact (Ellen) VZV. The morphology of the TGN in cells infected with gI_{Δ} and $gI_{\Delta N}$ cannot be distinguished from that of cells infected with $gI_{\Delta C}$. (A) Vesicles, cisternae, and vacuoles of the TGN are distorted in contour, and their membranes are increased in electron density (arrows) and apparent thickness. (B) The apparent increase in the thickness of the distorted membranes of the TGN vacuolar structures is due to the presence of a circumferential coating of dense tegument-like material. Some of the coated membrane-enclosed sacs of the TGN have flattened into cisternae and appear to adhere to one another (slightly curved arrow). Note also the proliferation of smooth cellular membranes, which are in continuity with the RER (sharply curved arrow). (C) The adherence of adjacent coated membrane-enclosed cisternae gives rise to bizarre concentric rings of repeating sacs. Electron-dense coatings are found between adjacent cisternae, while their lumens are electron lucent, giving rise to alternating light (lumen) and dark (coated membrane) stripes. (D) In a highly infected cell, the TGN has taken on the appearance of a honeycomb. The walls of the chambers of the honeycomb are composed of membranes the cytosolic faces of which are coated with an electron-dense material. Pleomorphic virions (arrows) can be found within some of the chambers. Bars, 150 nm.

Coincident expression of gE and ORF10p occurs in infected cells and is not significantly affected by deleting gI or its N- and C-terminal domains. ORF10p was found to be colocalized with gE in the TGN of cells infected with intact VZV (Fig. 9A to C). Since the structure of the TGN is altered in cells that are infected with gI mutant forms of VZV, we determined the effect of these mutations on the coincident distribution of ORF10p with gE in infected cells. Very little effect was found. In all three gI mutants, gI_{Δ} (Fig. 9D to F), $gI_{\Delta C}$ (Fig. 9G to I), and $gI_{\Delta N}$ (Fig. 9J to L), ORF10p continued to be colocalized with gE in the TGN. There were, however, occasional cells, seen especially in those infected with the gI_{Δ} mutant, in which gE immunoreactivity could be found in the TGN, but not ORF10p. In all cells, those infected with intact VZV (Fig. 9B), as well as those infected with the gI_{Δ} (Fig. 9E), $gI_{\Delta C}$ (Fig. 9H), and $gI_{\Delta N}$ (Fig. 9K) mutant virions, the cytosol was also moderately ORF10p immunoreactive.

At the electron microscopic level, ORF10p immunoreactiv-

ity was found in the cytosol of infected cells and, in cells infected with intact VZV, was also associated with the osmiophilic coats of membranes in the Golgi stack (Fig. 10A). In addition to its presence in Golgi regions, ORF10p immunoreactivity was found in the osmiophilic tegument of the mature virions that accumulated in the late endosomes-prelysosomes of cells infected with intact VZV (Fig. 10B). In cells infected with the gI mutant forms of VZV, the abnormal rings and stacks of membranes of the TGN were ORF10p immunoreactive (Fig. 10C). Again, the immunogold particles tended to lie over the dense osmiophilic material that coated these membranes. In cells that were heavily infected with the gI mutant virions, both the osmiophilic coatings of the membranes lining the chambers of the "honeycombs" that formed in the region of the TGN and the virions within these chambers contained ORF10p immunoreactivity (Fig. 10D).

Two additional viral proteins that are known to be components of tegument, IE62 (16, 17) (not illustrated) and IE63 (8,

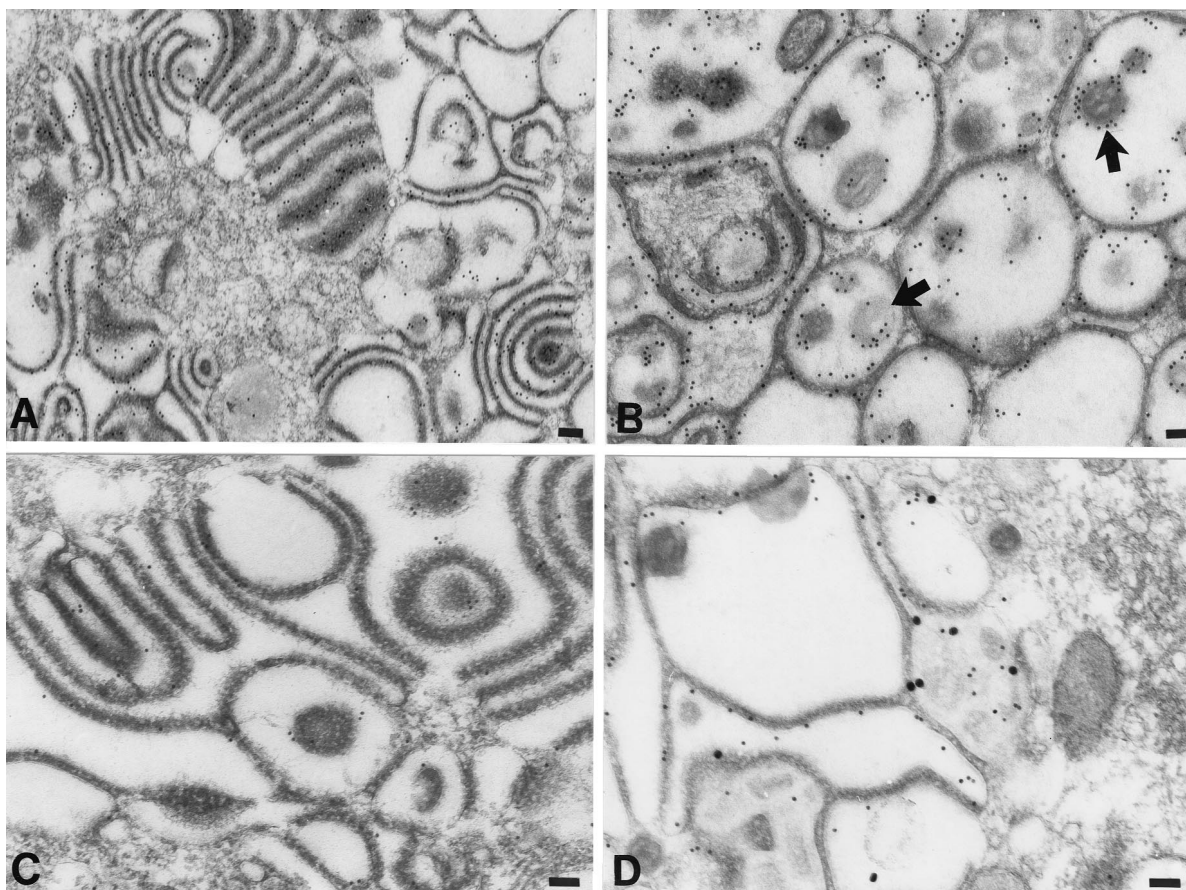


FIG. 6. The membranes of adherent sacs in the TGN of cells infected with the $gI_{\Delta C}$ mutant virus display both gE and gI immunoreactivities. (A and B) gE immunoreactivity, demonstrated with 10-nm particles of immunogold in the region of the TGN. (A) Gold particles are concentrated in the membranes of adjacent sacs and are not found in the cytosol. (B) The honeycomb-like structure (see Fig. 5D) found in the region of the TGN of a heavily infected cell contains gE immunoreactivity. Both of the membranes that delimit the chambers of the honeycomb and the virions within the cavities of the chambers are gE immunoreactive. The peripheral distribution of the gE immunoreactivity around the virions (B, arrows) indicates that gE is located in the viral envelope. (C) gI immunoreactivity, demonstrated with 10-nm particles of immunogold in the region of the TGN. Gold particles are concentrated in the membranes of adjacent sacs. The immunoreactivity of gI is less abundant than that of gE (compare with panel A). (D) gE immunoreactivity, demonstrated with 10-nm immunogold particles and gI immunoreactivity demonstrated simultaneously with 20-nm immunogold particles. The gE and gI immunoreactivities are each located in the same membranes lining the chambers of the honeycomb found in the TGN of a highly infected cell. Bars, 150 nm.

12, 15) (Fig. 11) were investigated. The immunoreactivities of both proteins were found to be strikingly nuclear (IE62, not illustrated; IE63, Fig. 11). Neither was detectably concentrated in the TGN of cells infected with intact VZV (Fig. 11A and B) or the gI_{Δ} (Fig. 11C and D), $gI_{\Delta C}$ (Fig. 11E and F), or $gI_{\Delta N}$ (Fig. 11G and H) mutants.

Interactions of gI and gE. Because of the complex formed between gI and gE at their N-terminal domains (14), the two glycoproteins usually traffic together (21, 30, 31). Since both gI (31) and gE (37) independently contain their own unique TGN targeting signals, the coexpression of either one of these proteins in a full-length nonmutated form would be expected to compensate for the loss of the TGN targeting signal in its partner. Binding of gI to gE in cells infected with $gI_{\Delta C}$ mutant virions thus might account for the TGN targeting of gI immunoreactivity that occurs in the face of the absence of the C-terminal TGN targeting signal of gI. To evaluate the ability of gE and gI to compensate for the loss of one another's TGN targeting signal, Cos-7 cells were cotransfected with cDNA

encoding a full-length form of one of these proteins and a truncated C-terminal mutant form of the other. The truncated form of gE has previously been reported to be retained in the RER of transfected Cos-7 cells and, to a lesser extent, also to be secreted (35). In Cos-7 cells that expressed only truncated gE, the gE immunoreactivity was found, as expected, to be restricted to the RER (Fig. 12A); however, when cells were cotransfected and expressed both the truncated gE and the full-length gI, gE immunoreactivity was now well concentrated in the TGN (Fig. 12B). Transfected Cos-7 cells that expressed truncated forms of gI, which lacked the T^{338} residue in the cytosolic domain that is essential for TGN targeting (31), retained most of the expressed protein in the RER (Fig. 12C). In contrast, when these cells were cotransfected and coexpressed a full-length gE with the truncated gI, then gI immunoreactivity was concentrated in the TGN (Fig. 12D). There were, however, limits to the extent to which gE could complement the loss of gI targeting. When the cytosolic domain of gI was completely deleted, gI immunoreactivity remained in the TGN

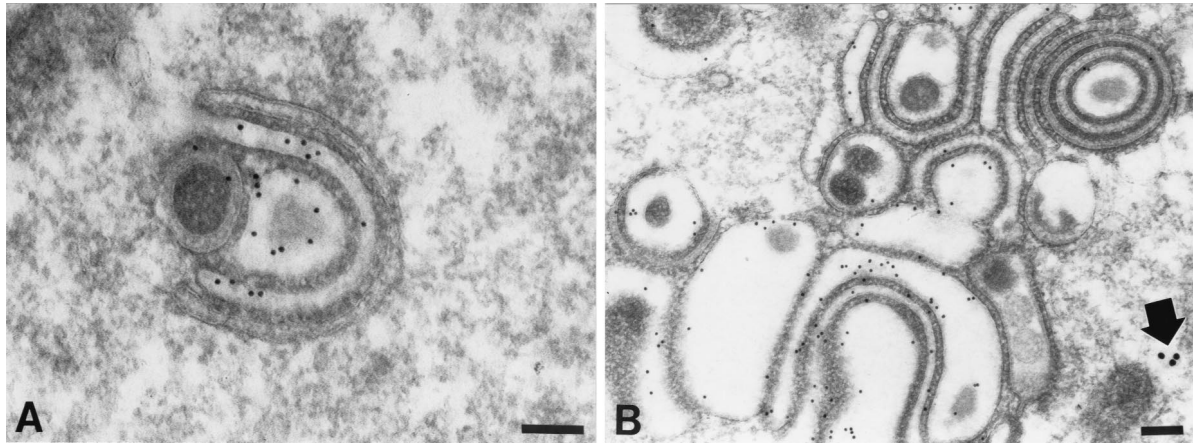


FIG. 7. gE immunoreactivity demonstrated with 10-nm immunogold particles and gI immunoreactivity demonstrated simultaneously with 20-nm immunogold particles in the TGN of a cell infected with the $gI_{\Delta AN}$ mutant virus. (A) The C-shaped TGN cisternae display the immunoreactivity of gE but not that of gI. (B) The membranes of concentric rings and adherent sacs in the TGN are gE immunoreactive. The gI immunoreactivity (arrow) is sparse and, when found, appears only in the cytosol. Bars, 150 nm.

(Fig. 12E and G), even when coexpressed with gE (Fig. 12E). The truncated gI retained in the RER, however, did not interfere with the TGN targeting of gE (Fig. 12F). These observations suggest that the TGN targeting information contained in

the sequence of gI enables gI to compensate for missing targeting information in gE and even to prevent the RER retention of a mutated form of gE that lacks both cytosolic and transmembrane domains. Similarly, gE can compensate for the

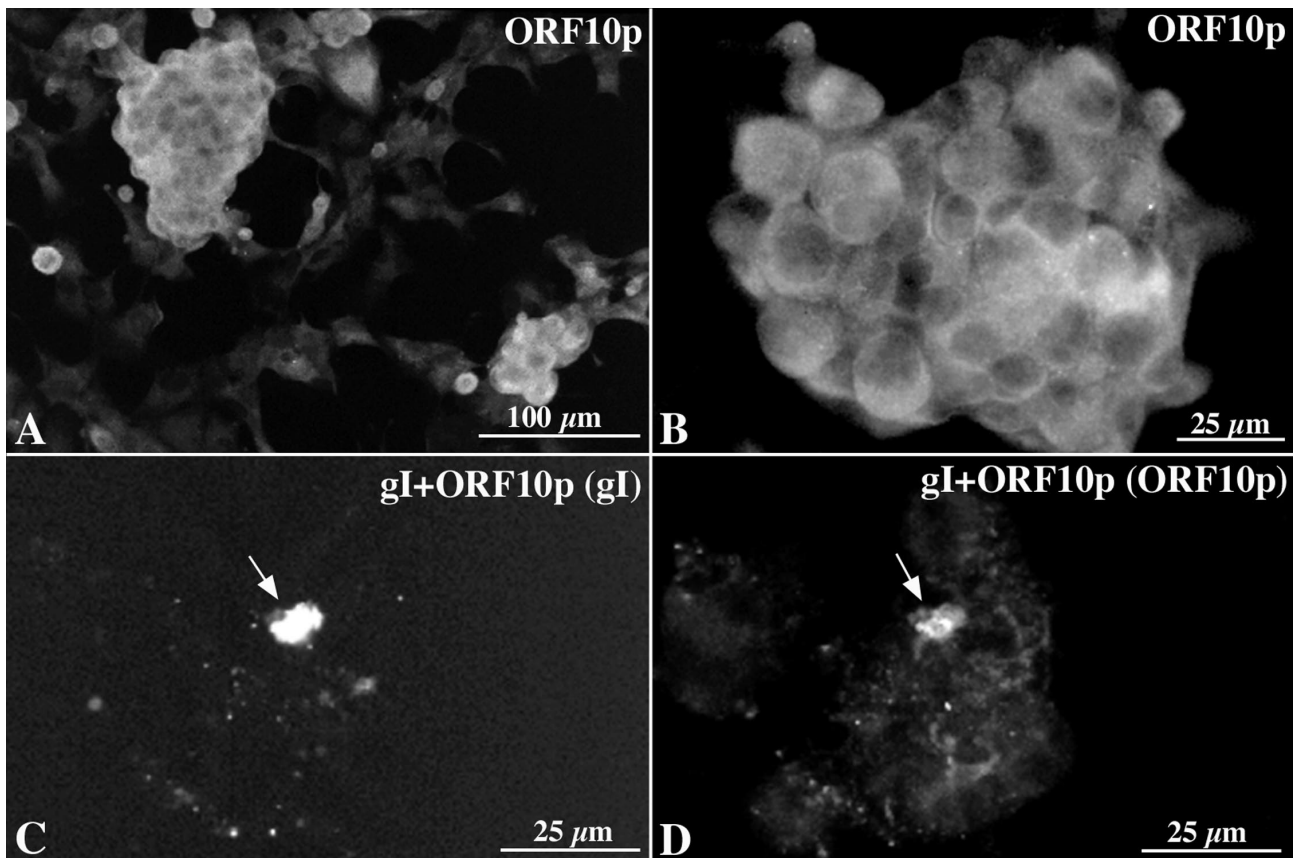


FIG. 8. ORF10p immunoreactivity is translocated to the TGN when coexpressed with gI. (A and B) ORF10p immunoreactivity in transfected Cos-7 cells expressing ORF10p by itself. The immunoreactivity is diffuse and cytoplasmic. (C and D) gI and ORF10p immunoreactivities in a cell that has been cotransfected with cDNA encoding gI and ORF10p. (C) The cell has been illuminated to show the Cy3 fluorescence of gI immunoreactivity. (D) The cell has been illuminated to show the FITC fluorescence of ORF10p immunoreactivity. The arrows point to the TGN where gI and ORF10p immunoreactivities have become colocalized. Bars: A, 100 μm ; B to D, 25 μm .

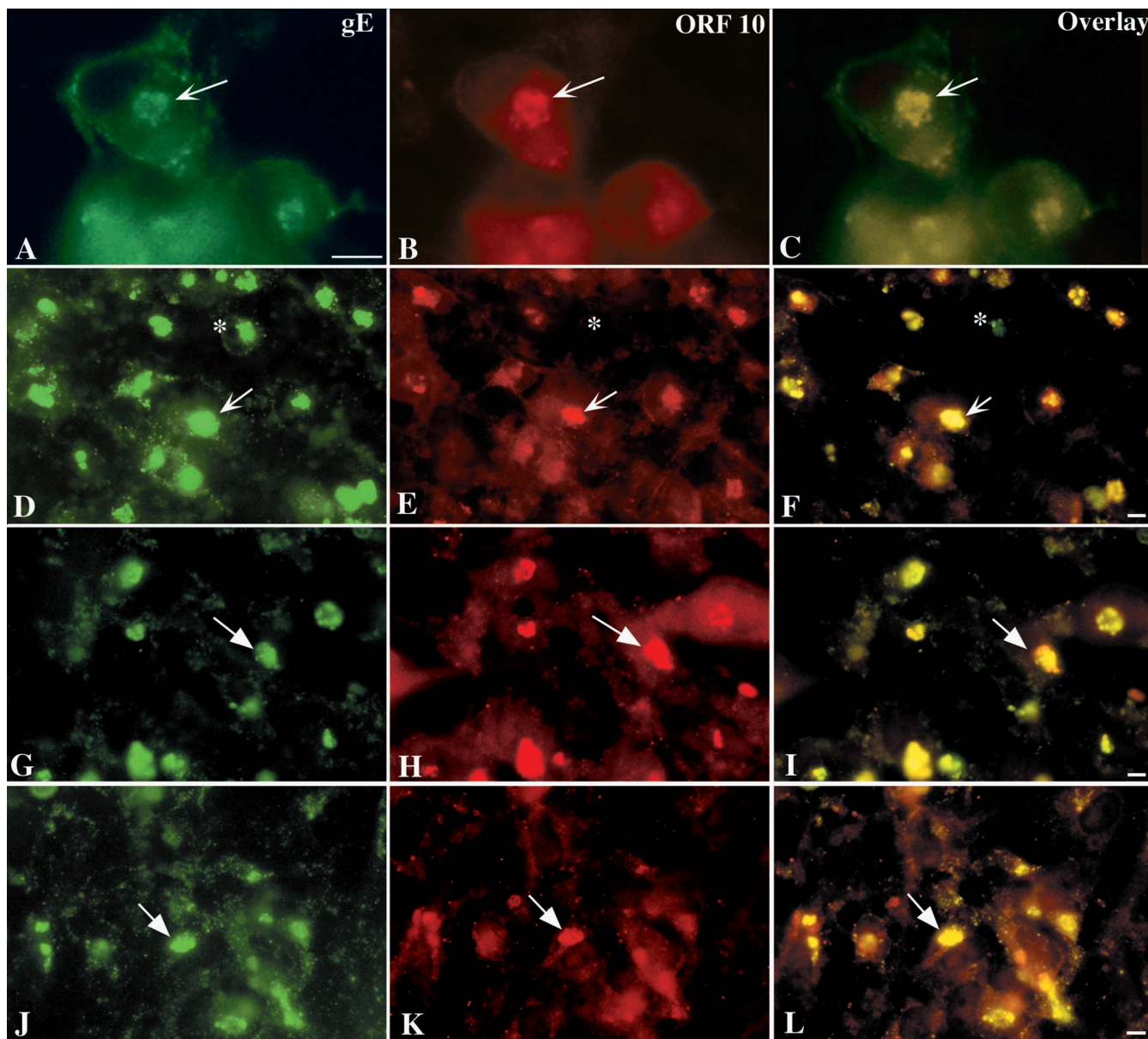


FIG. 9. gE and ORF10p immunoreactivities colocalize in the TGN of cells infected with intact (Ellen) or gI_{Δ} , $gI_{\Delta C}$, or $gI_{\Delta N}$ mutant forms of VZV. (A to C) Intact (Ellen) VZV. (D to F) gI_{Δ} mutant VZV. (G to I) $gI_{\Delta C}$ mutant VZV. (J to L) $gI_{\Delta N}$ mutant VZV. The column at the left (A, D, G, and J) illustrates gE immunoreactivity; the column in the center (B, E, H, and K) illustrates ORF10p immunoreactivity, and that at the right (C, F, I, and L) depicts the gE-ORF10p overlay. The arrows show the location of the TGN and the markers indicate 10 μ m.

loss of targeting information in gI, although gE cannot do so if gI lacks its entire cytosolic domain. The ability of gE to reach the TGN when a severely truncated gI with which it is coexpressed is retained in the RER suggests that the gE-gI complex formed at the N-terminal domains of these molecules is either conditional in its formation or able to be broken.

DISCUSSION

Experiments were carried out with mutant forms of VZV lacking either gI or the N- or C-terminal regions of gI in order to evaluate the role(s) played by gI in the final envelopment of VZV in the TGN. Since gE is known to form a complex with

gI in the RER, the effect of gE on the trafficking of gI was also assessed. Because both gE (3, 36, 37) and gI (31) each contain TGN targeting signals, we analyzed the ability of a full-length form of one of these proteins to compensate in TGN sorting for the absence of a targeting signal in the other. Finally, we tested the hypothesis that tegument proteins become incorporated into enveloping virions in the TGN by interacting with viral glycoproteins.

In cells that were infected with intact VZV, the immunoreactivities of gE and gI were concentrated coincidentally in the TGN. The complete deletion of gI (gI_{Δ}) in mutant VZV did not change the TGN localization of gE, although no gI immunoreactivity could be detected in cells infected with the gI_{Δ}

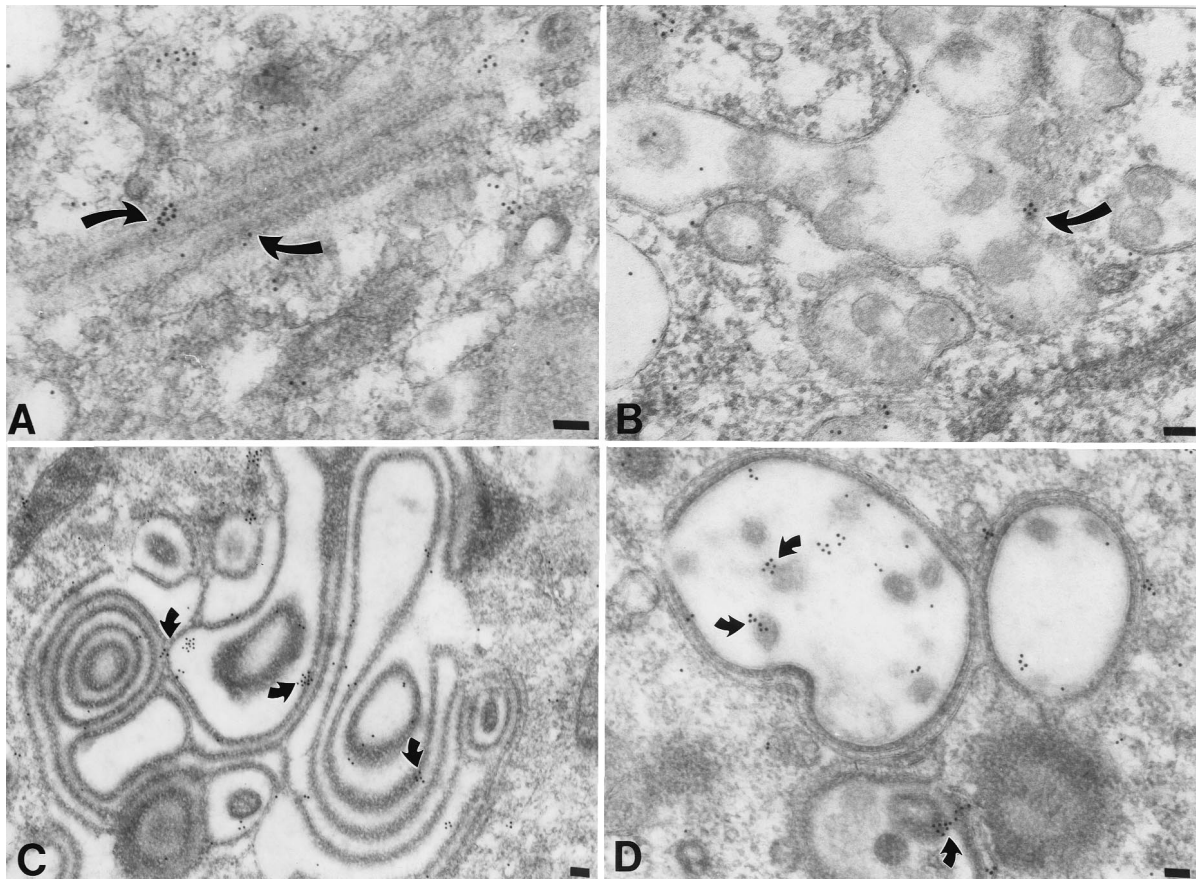


FIG. 10. ORF10p immunoreactivity is found in the cytosol, in coatings of Golgi-TGN membranes, and in virions in cells infected with VZV. (A) Intact (Ellen) VZV. ORF10p immunoreactivity is demonstrated with 10-nm particles of immunogold in the region of the Golgi apparatus. Gold particles are found in the cytosol and in the dense material coating membranes of the Golgi stack (arrows). (B) Late endosomes-prelysosomes in a cell infected with intact (Ellen) VZV. ORF10p immunoreactivity is found within pleomorphic virions (arrow) that accumulate within these vacuoles. (C) $gI_{\Delta N}$ mutant virus. ORF10p immunoreactivity is found in the osmiophilic material (arrows) that coats the membranes of the rings and stacks of adherent cisternae that characterize the TGN of cells infected with gI mutant virions (see Fig. 5). (D) $gI_{\Delta N}$ mutant virus. ORF10p immunoreactivity is found in the virions within the chambers (arrows) and the coating of the membranes that form the walls of the chamber of the honeycomb that characterizes the TGN of cells heavily infected with gI mutant virions. Bars, 150 nm.

mutant VZV. There appeared, however, to be somewhat less gE immunoreactivity on the surfaces of cells infected with gI_{Δ} . This observation is consistent with the suggestion that gI helps to retain gE in the plasma membrane (31). The endocytosis of gE (23) may normally be inhibited by binding to gI . Several investigators have reported that gI is not internalized from the cell surface in cells that express gI by itself even though the same cells internalize gE (1, 31; but see also reference 21). When the C-terminal domain of gI was deleted ($gI_{\Delta C}$), gE and gI immunoreactivities continued to colocalize in the TGN. Specifically, the immunoreactivities of both proteins were found in the same TGN membranes, and these membranes were coated with tegument-like material. Since the $gI_{\Delta C}$ mutant lacks both a TGN targeting signal and even a transmembrane domain, its concentration in membranes of the TGN is best explained by its binding to the N-terminal domain of gE . The truncated gI can thus be carried to the TGN as a passenger with gE , which because of its anchorage in membranes and targeting signal can act as a navigator. These data are thus consistent with the ideas that a gE - gI complex cotrans-

lationally, or at least before gI is sorted, would enable gE to capture the presumably soluble N-terminal domain of gI_{Δ} in the cisternal lumen, enable the gI ectodomain to exit the RER, and prevent it from being sorted to the secretory pathway. The deletion of the N-terminal domain of gI ($gI_{\Delta N}$) eliminates the signal sequence directing biosynthesis to ribosomes attached to the RER. Consequently, at the light microscopic level, almost no gI immunoreactivity could be detected in cells infected with the $gI_{\Delta N}$ mutant, while at the electron microscopic level, only sparse gI immunoreactivity was seen, and that immunoreactivity was confined to the cytosol. The ability of the antibodies to detect $gI_{\Delta N}$ at the electron microscopic level indicates that the relative scarcity of gI immunoreactivity in the cells infected with $gI_{\Delta N}$ is not the result of a failure of the antibodies to detect the protein. The paucity of $gI_{\Delta N}$, moreover, is consistent with the idea that the mutant protein is synthesized in the cytosol. Aberrant proteins synthesized in the cytosol are rapidly degraded (29, 38). In the absence of its N-terminal domain, therefore, gI evidently becomes a cytosolic protein and does not interact with gE . The $gI_{\Delta N}$ mutant probably is virtu-

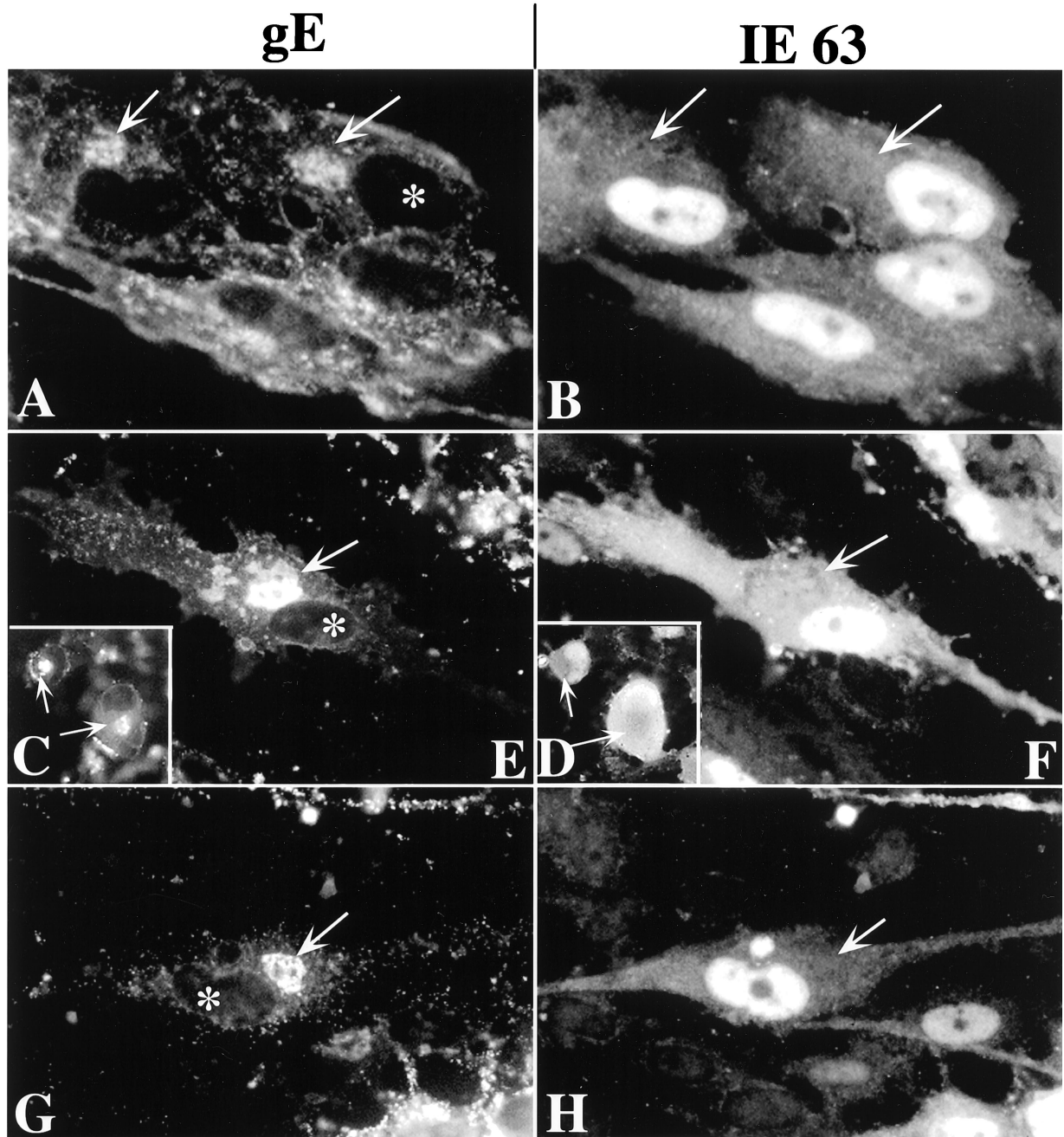


FIG. 11. IE63 immunoreactivity does not colocalize with that of gE in the TGN of VZV-infected cells. (A and B) Intact (Ellen) VZV. (C and D [insets]) gI_{Δ} mutant VZV. (E and F) $gI_{\Delta C}$ mutant VZV. (G and H) $gI_{\Delta N}$ mutant VZV. The column at the left (A, C, E, and G) illustrates gE immunoreactivity, and that at the right (B, D, F, and H) illustrates IE63 immunoreactivity. The arrows show the location of the TGN. The asterisk shows the location of the nucleus in infected cells in which gE immunoreactivity has been demonstrated. There is no nuclear gE immunoreactivity and no concentration of IE63 immunoreactivity in the TGN, although some diffuse cytoplasmic IE63 immunoreactivity can be discerned. The nuclei of infected cells are highly IE63-immunoreactive. Bars, 10 μ m.

ally identical to the gI_{Δ} mutant, in that the virions produced by cells infected with either one probably lack any form of gI.

Although mutations in gI did not prevent the TGN targeting of gE, each of the gI_{Δ} , $gI_{\Delta C}$, and $gI_{\Delta N}$ mutations exerted an identical effect on the morphology of the TGN. This effect was to cause the membranes of TGN sacs to become completely coated on their cytosolic faces with electron-dense material

that resembled tegument and to adhere to one another (Fig. 13). The TGN sacs in cells infected with gI mutant forms of VZV did not form the C-shaped wrapping cisternae that envelop VZV in cells infected with intact VZV. The major difference between the TGN cisternae of cells infected with intact VZV and those of cells infected with the gI mutant virions was the strikingly asymmetric distribution of the tegument-like coat

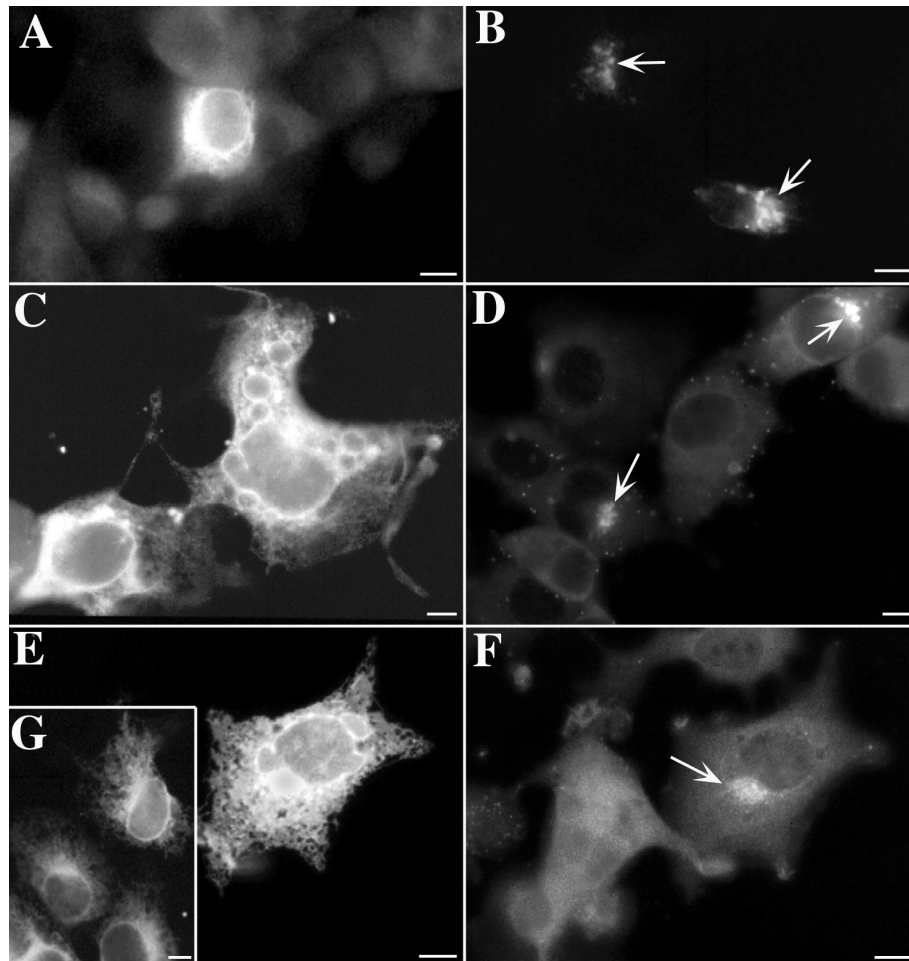


FIG. 12. In cotransfected cells, the intracellular transport and targeting of truncated forms of gI and gE can be influenced by coexpression of full-length forms of the other protein. (A) gE immunoreactivity is found in an ER pattern in cells expressing a truncated form of gE, which lacks transmembrane and cytosolic domains. (B) gE immunoreactivity is concentrated in the TGN (arrows) when cells coexpress the truncated gE with a full-length gI. (C) gI immunoreactivity is found in an ER pattern in cells expressing a truncated form of gI, which lacks the T³³⁸ targeting signal and the portion of the cytosolic domain C-terminal to it. The sequence of the cytosolic domain of this mutant is SVKRRRIKKHPYRPNTK TRRGIQNATPESDVMLEAAIAQLA. (D) gI immunoreactivity is concentrated in the TGN (arrows) when cotransfected cells express both the truncated form of gI shown in C and a full-length form of gE. (E and G) gI immunoreactivity is found in an ER pattern in cells expressing a severely truncated form of gI, which lacks the entire cytosolic domain of the molecule. The cell in panel E has been cotransfected and expresses a full-length form of gE, which has not influenced the ER retention of gI. (F) Same cell shown in panel E, now illuminated to demonstrate gE immunoreactivity. Despite the retention of gI immunoreactivity in the ER, the immunoreactivity of gE has reached the TGN (arrow) and is concentrated in this organelle. (G) gI immunoreactivity is found in an ER pattern in transfected cells expressing only the severely truncated form of gI, which lacks the entire cytosolic domain. Bars, 10 μ m.

on the cisternae when cells were infected with intact virions (Fig. 13, upper panel). In contrast to the complete coating that occurred when cells were infected with gI mutant virions, that associated with intact VZV was sharply limited to the concave face of flattened cisternae that invaginated to assume the shape of a "C". In the cells infected with intact VZV, moreover, individual sacs remained segregated and wrapped singly around nucleocapsids, trapping them on the tegument-coated invaginated face of the wrapping cisternae. The symmetrically coated sacs of the TGN of cells infected with gI mutant virions were not seen to wrap around nucleocapsids in this fashion and instead adhered to one another, as if the tegument coating were "sticky" and glued them together (Fig. 13, lower panels). The consequence of the adherence of adjacent TGN sacs in cell infected with gI mutant forms of VZV was the gross

distortion of the TGN, giving rise to stacks and concentric rings of cisternae and, ultimately, in heavily infected cells, forming a massive honeycomb in the Golgi region. The defect in the TGN cisternae in gI mutant virions interfered with the envelopment of VZV and prevented the intracellular transport of newly enveloped VZV to post-Golgi structures, such as late endosomes-prelysosomes and exocytotic vesicles.

It seems likely that the defective arrangement of tegument coating the membranes of TGN cisternae in cells infected with gI mutant forms of VZV reflects a similar defect in the segregation of viral glycoproteins within the plane of the membrane. In order to utilize the concave membrane to form a viral envelope, it is necessary for all of the viral glycoproteins to be concentrated in that domain. If tegument proteins then adhere (directly or via adaptors) to the cytosolic tails of the localized

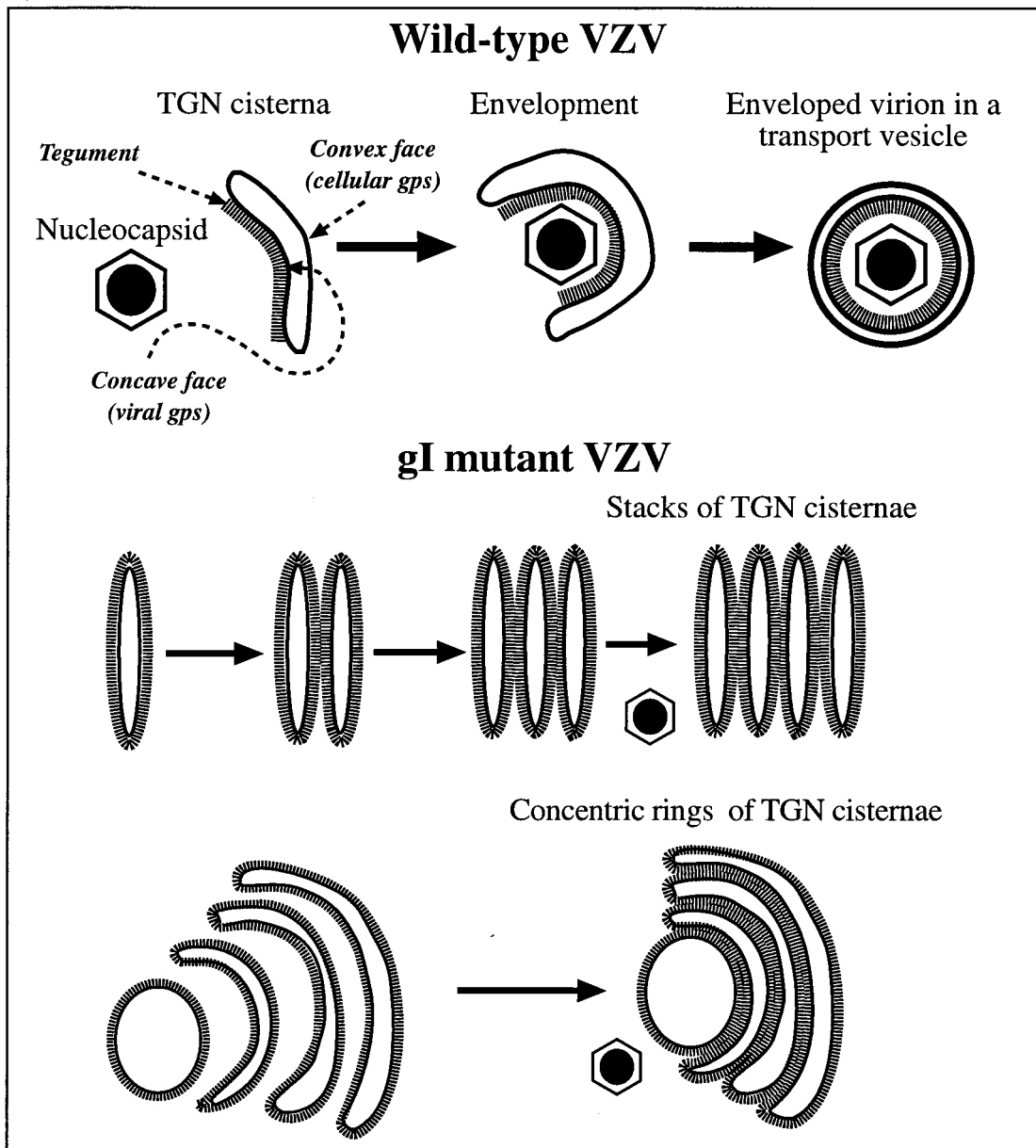


FIG. 13. A heuristic model depicting the role of TGN cisternae in viral envelopment in cells infected with intact (Ellen) VZV and how the envelopment process becomes defective in cells infected with gI_{Δ} , $gI_{\Delta C}$, or $gI_{\Delta N}$ mutant virions. When cells are infected with intact (Ellen) VZV (upper panel), nucleocapsids that are free in the cytosol become associated with specialized wrapping cisternae in the TGN. These cisternae are curvilinear, with distinct concave and convex faces. Tegument adheres to the concave face of the curving cisternae, and as the arms of the wrapping cisternae approach one another and ultimately fuse, tegument and the nucleocapsid are enclosed within. The membrane of the concave face of the wrapping cisternae, which is proposed to be rich in viral glycoproteins, becomes the viral envelope. The membrane of the convex face, which is rich in cellular proteins, such as Man 6-P receptors, delimits a transport vesicle that encloses the newly enveloped virion. When gI is deficient (lower panels), viral proteins are no longer segregated to one face of the TGN cisternae. As a result the tegument, which is presumed to bind to the cytosolic domains of the viral glycoproteins, is not confined to a single surface of the TGN cisternae. Because tegument is not restricted to the concave face of curving cisternae, adjacent tegument-coated cisternae fuse with one another to give rise to stacks and concentric rings of adherent sacs. The defect in the TGN interferes with viral envelopment and with the post-Golgi transport of VZV.

glycoproteins, the tegument will also, of necessity, be restricted to the concave face of the enveloping cisternae. The concave TGN membranes have been demonstrated to contain gE immunoreactivity and the tegument that adheres to them reacts with antibodies to VZV (10). Similarly, the convex membrane of the TGN cisternae contains Man 6-P receptors (10) and would be expected also to be rich in other cellular proteins

involved in vesicular sorting and fusion but poor in viral glycoproteins. Indeed, the convex face of the wrapping sac lacks gE immunoreactivity and does not react with antibodies to VZV. The current observation that ORF10p, which is known to be a component of viral tegument (5, 6), colocalizes in the TGN with gE , supports the idea that tegument interacts with viral glycoproteins. Tegument proteins lack a signal sequence

and, of necessity, are synthesized in the cytosol. This explains why ORF10p is diffusely located in the cytoplasm in transfected cells that express it. By interacting with the cytosolic domains of viral glycoproteins, tegument proteins, such as ORF10p, can concentrate in the TGN at the site of viral envelopment and be incorporated into viral particles. This idea that tegument proteins do so is strongly supported by the observation that gI, which contains a TGN retention signal, causes ORF10p to translocate from the cytosol to the TGN in cotransfected cells that express both proteins. Segregation of viral from cellular glycoproteins within TGN cisternae evidently fails in the gI mutant virions. This failure causes gE and tegument to become evenly distributed around the TGN cisternae. We postulate that tegument interacts with glycoproteins and thus reflects their distribution. Other glycoproteins are probably affected by the gI mutations in a manner similar to gE, but this has not yet been demonstrated. All of the glycoproteins, however, must be present in the membrane that becomes the viral envelope (because all are present in the viral envelope). It thus seems likely that the loss of the segregated concave face of the TGN "wrapping" cisternae in cells infected with the gI mutants reflects the maldistribution of more glycoproteins than just gE.

The coating of tegument appears to be sticky if coated membranes come into apposition with one another. Adjacent coated sacs thus adhere (Fig. 13), giving rise to the stacks and rings of TGN sacs in the cells infected with mutant virions. Evidently, adherence of adjacent sacs is rare when tegument and viral glycoproteins are confined to the concave domains of the enveloping cisternae of cells infected with intact VZV. gI would thus appear to play a necessary role in the segregation of viral and cellular glycoproteins in the cisternae of the TGN that provide VZV with its definitive envelope.

The role of gI in segregating viral glycoproteins, and thus in envelopment, depends on the C-terminal domain of the glycoprotein. As a result, the function of gI in maintaining the appropriate structure of the enveloping cisternae of the TGN was lost from all three gI mutant virions. The effect of the gI_Δ and the gI_{ΔN} mutants are readily understandable, because in cells infected with either one, essentially no gI reaches the membranes of the TGN. In the latter case, the N-terminal deletion prevents biosynthesis of the mutated gI in the RER and thus renders it a cytosolic protein, accounting for the absence of gI immunoreactivity from the TGN or its membranes in cells infected with gI_{ΔN}. The mutated protein made by cells infected with the gI_{ΔC} mutant, however, does reach the TGN, where it is colocalized in TGN membranes with gE. Two possibilities can be envisioned for the failure of gI that lacks a C-terminal to support cell-VZV protein segregation and viral envelopment. One is that a sequence within the C-terminal domain of gI is critical for these functions of gI. The putative C-terminal sequence may be needed to interact with cytosolic cellular proteins that restrict the motility of VZV glycoproteins within the plane of the TGN cisternal membrane or to interact with other VZV glycoproteins to form rafts that stay within the concave domain. A second possibility, which is not mutually exclusive with the first, is that gI is only effective in bringing about the segregation of proteins when it is itself an integral membrane protein. The C-terminal deletion of the gI_{ΔC} mutant removes both the transmembrane and the cytosolic domains of the protein, and thus gI_{ΔC} is presumably a soluble

protein within the lumen of the RER. gI_{ΔC} is carried as a passenger to the TGN because it binds to gE. Whatever the reason why gI is required for maintaining the integrity of enveloping membranes within the TGN, this requirement also makes gI critical for normal viral envelopment. In the absence of a functional gI protein, the gI mutant virions are unable to exit from the TGN, unable to reach post-TGN structures, and thus unable to be released from cells as enveloped virions.

Despite the critical roles played by the C-terminal domain of gI, the deletion of gI is not lethal to VZV (4, 20). Infected cells, even those lacking gI, contain free nucleocapsids in the cytosol and fuse with adjacent cells. Cell fusion permits nucleocapsids to pass from one cell to another and thus enables infection to be transmitted *in vitro*, even though envelopment of VZV does not occur. The post-Golgi delivery of enveloped virions to late endosomes-prelysosomes causes severe degradation of VZV to occur prior to its release from infected cells (10), so that the ambient medium in which infected cells are suspended is virtually noninfectious (32). The mechanism by which infection spreads *in vitro* from cells infected with gI mutant forms of VZV is thus probably not very different from that which occurs from cells infected with intact VZV, although cell-to-cell spread is less efficient in the case of the gI mutants (20).

Even though gI can cause ORF10p to become concentrated in the TGN, gI is not essential for this to occur. ORF10p was found to colocalize with gE in the TGN in cells infected with the gI_Δ, gI_{ΔC}, and gI_{ΔN} mutants equally well as in cells infected with intact VZV. These observations suggest that other glycoproteins besides gI interact with ORF10p. Alternatively, ORF10p may interact with other tegument proteins in infected cells that serve as adapters that anchor ORF10p to a glycoprotein other than gI. The immunolocalization of ORF10p on the cytosolic face of TGN membranes, as well as its proximity to gE, is consistent with the idea that ORF10p interacts, directly or via an adapter, with the cytosolic domain of one or more of the other glycoproteins. The concentration of ORF10p in the TGN, moreover, does not depend on the maintenance of the structural integrity of enveloping cisternae. Like other tegument proteins, it concentrates even in the bizarre TGN found in cells infected with gI mutant virions. It is not clear why IE62 and IE63 did not, like ORF10p, become concentrated in the TGN. Both are thought to be components of virions and thus would be expected to be present at the site of VZV envelopment within the TGN. It is possible that both IE62 and IE63 actually are present in the region of the TGN, but at a concentration that is not detectably higher than that of the surrounding cytosol. Only a concentration in the TGN that exceeds that of the neighboring cytoplasm would be recognized immunocytochemically as localized to the TGN. A concentration of IE62 and IE63 in the TGN that is the equal to that of the cytosol may be adequate for incorporation of these proteins into newly enveloped virions. Alternatively, IE62 is mainly nuclear early in infection and does not become concentrated in the cytoplasm until later (16). It is thus possible that IE62 was not seen in the cytoplasm because the cells were investigated while it was primarily nuclear. Both IE62 and IE63 function primarily in the nuclei of infected cells; a lower cytoplasmic concentration of IE62 and IE63 may still be adequate for viral envelopment.

Both gE (2, 36, 37) and gI (31) contain TGN targeting

information within their sequences. The two proteins also interact with one another (1, 13, 14, 21, 24). One role for this interaction may be to provide a fail-safe mechanism that ensures that appropriate quantities of gE and gI are delivered to the TGN even if mistakes are made by cells in reading the signals of one or the other glycoprotein. gE will thus target gI to the TGN if gI is mutated and lacks a targeting signal (1, 31), and we have now found that gI will do the same for gE if gE is mutated and lacks the requisite TGN targeting information. The sorting of gE and gI is accomplished by different mechanisms. gE is retrieved from the plasma membrane by endocytosis (23), and the gE-containing endosomes are routed to the TGN (2, 36, 37). In contrast, gI is partially retained in the TGN following its passage through the Golgi stack, and when the gI that is not retained in the TGN reaches the plasma membrane, it remains there unless retrieved as a complex with gE (1, 31). gI has been reported to be internalized in HeLa cells due to a methionine-leucine motif in its cytosolic domain, but there is no evidence that even this internalized gI is transported back to the TGN (21). The complex formed by gE and gI may thus slow the exit of gE from the TGN in the first place and help to prevent the disappearance of gE from the plasma membrane due to endocytic retrieval in the second. The gE-gI complex may also function, provided gI is anchored in the membrane, in helping to maintain the association of glycoproteins in a restricted domain of enveloping membranes of the TGN.

In summary, we show here that gI is necessary for the maintenance of enveloping cisternae in the TGN of cells that have been infected with VZV. In particular, the C-terminal end of gI is critical for this function. We suggest that the segregation of viral and cellular proteins that must take place within the plane of TGN membranes does not occur in the absence of the C-terminal domain of gI or of a membrane-anchored gI protein. As a result, the glycoproteins spread uniformly to all surfaces of the TGN wrapping cisternae and, as a consequence, so too does the coating of tegument with which the viral glycoproteins interact. Apposed tegument-coated surfaces are associated with the adherence of adjacent TGN cisternae, forming stacks and concentric rings of coated sacs. The TGN abnormality interferes with viral envelopment and blocks the transport of enveloped virions to post-Golgi structures. We also show that ORF10p, a tegument protein, is translocated from the cytosol to the TGN when it is coexpressed with gI. ORF10p also becomes concentrated on the cytosolic face of TGN membranes in infected cells, where it colocalizes in apposition to gE. ORF10p, therefore, interacts with gI, although the expression of gI is not essential for ORF10p localization in the TGN of infected cells. Although gI is dispensable for infection, therefore, it is indispensable for normal envelopment of VZV and for the secretion of enveloped virions. Future studies on the role of gI in the segregation of viral and cellular proteins may help in advancing the production of a recombinant VZV vaccine and in developing novel antiviral compounds.

ACKNOWLEDGMENT

This work was supported by NIH grant AI12718.

REFERENCES

- Alconada, A., U. Bauer, L. Baudoux, J. Piette, and B. Hoffack. 1998. Intracellular transport of the glycoproteins gE and gI of the varicella-zoster virus. *J. Biol. Chem.* **273**:13430–13436.

- Alconada, A., U. Bauer, and B. Hoffack. 1996. A tyrosine-based motif and a casein kinase II phosphorylation site regulate the intracellular trafficking of the varicella-zoster virus glycoprotein I, a protein localized in the trans-Golgi network. *EMBO J.* **15**:6096–6110.
- Alconada, A., U. Bauer, B. Sodeik, and B. Hoffack. 1999. Intracellular traffic of herpes simplex virus glycoprotein gE: characterization of the sorting signals required for its trans-Golgi network localization. *J. Virol.* **73**:377–387.
- Cohen, J., and H. Nguyen. 1997. Varicella-zoster virus glycoprotein I is essential for growth in Vero cells. *J. Virol.* **71**:6913–6920.
- Cohen, J., and K. E. Seidel. 1994. Varicella-zoster virus (VZV) open reading frame (ORF) 10 protein the homologue of the essential herpes simplex virus protein VP16, is dispensable for VZV replication in vitro. *J. Virol.* **68**:7850–7858.
- Cohen, J. I. 1999. Genomic structure and organization of varicella zoster virus, p. 10–20. *In* M. H. Wolff, S. Schünemann, and A. Schmidt (ed.), *Varicella-zoster virus: molecular biology, pathogenesis, and clinical aspects*, vol. 3. Karger, Basel, Switzerland.
- Dahms, N. M., P. Lbel, and S. Kornfeld. 1989. Mannose 6-phosphate receptors and lysosomal targeting. *J. Biol. Chem.* **264**:12115–12118.
- Debrus, S., C. Sadzot-Delvaux, A. F. Nikkels, J. Piette, and B. Rentier. 1995. Varicella-zoster virus gene 63 encodes an immediate-early protein that is abundantly expressed during latency. *J. Virol.* **69**:3240–3245.
- Gabel, C., L. Dubey, S. Steinberg, M. Gershon, and A. Gershon. 1989. Varicella-zoster virus glycoproteins are phosphorylated during posttranslational maturation. *J. Virol.* **63**:4264–4276.
- Gershon, A., Z. Zhu, D. L. Sherman, C. A. Gabel, R. T. Ambron, and M. D. Gershon. 1994. Intracellular transport of newly synthesized varicella-zoster virus: final envelopment in the trans-Golgi network. *J. Virol.* **68**:6372–6390.
- Griffiths, G., B. Hoffack, K. Simons, I. Mellman, and S. Kornfeld. 1988. The mannose 6-phosphate receptor and the biogenesis of lysosomes. *Cell* **52**:329–341.
- Jackers, P., P. Defechereux, L. Baudaux, C. Lambert, M. Massaer, M. P. Merville-Louis, B. Rentier, and J. Piette. 1992. Characterization of regulatory functions of varicella-zoster virus gene 63-encoded protein. *J. Virol.* **66**:3899–3903.
- Kimura, H., S. E. Straus, and R. K. Williams. 1998. Baculovirus expression, purification, and properties of varicella-zoster virus gE, gI, and the complex they form. *J. Infect. Dis.* **178**(Suppl. 1):S13–S15.
- Kimura, H., S. E. Straus, and R. K. Williams. 1997. Varicella-zoster virus glycoproteins E and I expressed in insect cells form a heterodimer that requires the N-terminal domain of glycoprotein I. *Virology* **233**:382–391.
- Kinchington, P. R., D. Bookley, and S. E. Turse. 1995. The transcriptional regulatory proteins encoded by varicella-zoster virus are open reading frames (ORFs) 4 and 63, but not ORF 61, are associated with purified virus particles. *J. Virol.* **69**:4274–4282.
- Kinchington, P. R., K. Fite, and S. E. Turse. 2000. Nuclear accumulation of IE62, the varicella-zoster virus (VZV) major transcriptional regulatory protein, is inhibited by phosphorylation mediated by the VZV open reading frame 66 protein kinase. *J. Virol.* **74**:2265–2277.
- Kinchington, P. R., J. Hougland, A. Arvin, W. Ruyechan, and J. Hay. 1992. The varicella-zoster virus immediate-early protein IE62 is a major component of virus particles. *J. Virol.* **66**:359–366.
- Kornfeld, R., and S. Kornfeld. 1985. Assembly of asparagine-linked oligosaccharides. *Annu. Rev. Biochem.* **54**:631–646.
- Kornfeld, S. 1987. Trafficking of lysosomal enzymes. *FASEB J.* **1**:462–468.
- Mallory, S., M. Sommer, and A. M. Arvin. 1997. Mutational analysis of the role of glycoprotein I in varicella-zoster virus replication and its effects on glycoprotein E conformation and trafficking. *J. Virol.* **71**:8279–8288.
- Olson, J., and C. Grose. 1998. Complex formation facilitates endocytosis of the varicella-zoster virus gE:gI Fc receptor. *J. Virol.* **72**:1542–1551.
- Olson, J. K., G. A. Bishop, and C. Grose. 1997. Varicella-zoster virus Fc receptor gE glycoprotein: serine/threonine and tyrosine phosphorylation of monomeric and dimeric forms. *J. Virol.* **71**:110–119.
- Olson, J. K., and C. Grose. 1997. Endocytosis and recycling of varicella-zoster virus Fc receptor glycoprotein gE: internalization mediated by a YXXL motif in the cytoplasmic tail. *J. Virol.* **71**:4042–4054.
- Olson, J. K., R. A. Santos, and C. Grose. 1998. Varicella-zoster virus glycoprotein gE: endocytosis and trafficking of the Fc receptor. *J. Infect. Dis.* **178**(Suppl. 1):S2–S6.
- Pagano, R. E., M. A. Sepanski, and O. C. Martin. 1989. Molecular trapping of a fluorescent ceramide analogue at the Golgi apparatus of fixed cells: interaction with endogenous lipids provides a trans-Golgi marker for both light and electron microscopy. *J. Cell Biol.* **109**:2067–2079.
- Schweitzer, A., S. Kornfeld, and J. Rohrer. 1998. Proper sorting of the cation-dependent mannose 6-phosphate receptor in endosomes depends on a pair of aromatic amino acids in its cytoplasmic tail. *Proc. Natl. Acad. Sci. USA* **94**:14471–14476.
- Seaman, M. N. J., P. J. Sowerby, and M. S. Robinson. 1996. Cytosolic and membrane-associated proteins involved in the recruitment of AP-1 adaptors onto the trans-Golgi network. *J. Biol. Chem.* **271**:25446–25451.

28. **Traub, L. M., and S. Kornfeld.** 1997. The trans-Golgi network: a late secretory sorting station. *Curr. Opin. Cell Biol.* **9**:527–533.
29. **Voges, D., P. Zwickl, and W. Baumeister.** 1999. The 26S proteasome: a molecular machine designed for controlled proteolysis. *Annu. Rev. Biochem.* **68**:1015–1068.
30. **Wang, Z., M. D. Gershon, O. Lungu, C. A. Panagiotidis, and A. Gershon.** 1998. Intracellular transport of varicella-zoster glycoproteins. *J. Infect. Dis.* **178**:S7–S12.
31. **Wang, Z.-H., M. D. Gershon, O. Lungu, Z. Zhu, and A. A. Gershon.** 2000. Trafficking of varicella-zoster virus glycoprotein, gI: T³³⁸-dependent retention in the *trans*-Golgi network, secretion and mannose 6-phosphate-inhibitable uptake of the ectodomain. *J. Virol.* **74**:6600–6613.
32. **Weller, T. H.** 1953. Serial propagation in vitro of agents producing inclusion bodies derived from varicella and herpes zoster. *Proc. Soc. Exp. Biol. Med.* **83**:340–346.
33. **Whealy, M. E., J. P. Card, R. P. Meade, A. K. Robbins, and L. W. Enquist.** 1991. Effect of brefeldin A on alphaherpesvirus membrane protein glycosylation and virus egress. *J. Virol.* **65**:1066–1080.
34. **Ye, M., K. M. Duus, J. Peng, D. H. Price, and C. Grose.** 1999. Varicella-zoster virus Fc receptor component gI is phosphorylated on its endodomain by a cyclin-dependent kinase. *J. Virol.* **73**:1320–1330.
35. **Zhu, Z., M. D. Gershon, C. Gabel, D. Sherman, R. Ambron, and A. A. Gershon.** 1995. Entry and egress of VZV: role of mannose 6-phosphate, heparan sulfate proteoglycan, and signal sequences in targeting virions and viral glycoproteins. *Neurology* **45**:S15–S17.
36. **Zhu, Z., M. D. Gershon, Y. Hao, R. T. Ambron, C. A. Gabel, and A. A. Gershon.** 1995. Envelopment of varicella zoster virus (VZV): targeting of viral glycoproteins to the trans-Golgi network. *J. Virol.* **69**:7951–7959.
37. **Zhu, Z., Y. Hao, M. D. Gershon, R. T. Ambron, and A. A. Gershon.** 1996. Targeting of glycoprotein I (gE) of varicella-zoster virus to the *trans*-Golgi network by a signal sequence (AYRV) and patch in the cytosolic domain of the molecule. *J. Virol.* **70**:6563–6575.
38. **Zwickl, P., D. Voges, and W. Baumeister.** 1999. The proteasome: a macromolecular assembly designed for controlled proteolysis. *Philos. Trans. R. Soc. Lond. B Biol. Sci.* **354**:1501–1511.